Frontier exploration and the North Atlantic Igneous Province: new insights from a 2.6 km offshore volcanic sequence in the NE Faroe-Shetland Basin

J.M. Millett[1,2], M.J. Hole[2], D.W. Jolley[2], N. Schofield[2], E. Campbell[3]

[1] *VBPR AS, Oslo Science Park, Gaustadalléen 21, N-0349 OSLO, NORWAY*

[2] *Department of Geology & Petroleum Geology, University of Aberdeen, Aberdeen AB24 3UE, UK*

[3] *Chevron Energy Technology Company, 1500 Louisiana Street, Houston, TX 77002-7308*

Abstract

The Lagavulin exploration well 217/15-1Z penetrated a ~2.6 km thick volcanic sequence dominated by extrusive basaltic rocks spanning the Palaeocene-Eocene boundary in the NE Faroe-Shetland Basin (FSB). The well comprises one of the thickest drilled sequences through the North Atlantic Igneous Province. Integrated analysis of drill cuttings and wireline-log data reveals key volcanic lithofacies: i) tabular lava flows; ii) compound lava flows; iii) hyaloclastite; and iv) volcaniclastic rocks. The volcanic facies reveal two major sub-aqueous to sub-aerial sequences consistent with lava delta progradation. These sequences are separated by a volcanic hiatus represented by extensive reddened soils which preceded the re-submergence of the area. Emergence followed by submergence of the first lava delta is interpreted to record an intra-T40 transient uplift event near the Palaeocene-Eocene boundary. Basalts from the lower ~1.3 km have low TiO_2 (<1.5 weight %) and low Zr/Y (2-3), with olivine-phyric picrites towards the base (Mg# 70-82; olivine Fo_{85-91}). The hiatus correlates precisely with a change to high TiO_2 (2.5-3.2 weight %) high Zr/Y (>4) compositions which dominate the upper sequence. The associated change in lava geochemistry, transient uplift and volcanic hiatus appears consistent with a transient pulse of hot buoyant plume material passing beneath the area.

Supplementary material: All raw geochemical data and supplementary analyses available at: http://www.geolsoc.org.uk/SUP0000

Introduction

The North Atlantic Igneous Province (NAIP) is one of the best-known and best-documented large igneous provinces (LIPs) on Earth (Thompson 1982; Saunders *et al.* 1997). There are however still vast areas of the province, now submerged deep beneath the North

Atlantic Ocean, from which very limited or no rock samples and associated data have been retrieved. Previous investigations of onshore and available offshore records have demonstrated that significant variations in the temporal and spatial distribution of volcanism (Planke *et al.* 2000; Jolley & Bell 2002a; Passey & Jolley 2009; Jolley *et al.* 2012; Hole *et al.* 2015) and magmatic sources (Saunders *et al.* 1997; Larsen *et al.* 1999; Barker *et al.* 2006) are present within the NAIP. New data from unexplored regions are therefore important if we are to progress our understanding of the complex spatial and temporal magmatic, volcanic and stratigraphic evolution of the NAIP.

On-going hydrocarbon exploration focused along the SE volcanic margin of the North Atlantic is now enabling access to the rocks of some of these until recently unexplored regions (Austin *et al.* 2014). A concomitant increase in seismic data coverage and resolution, allowing better remote imaging and interpretation of the subsurface volcanic sequences (e.g. Duncan *et al.* 2009; Wright *et al.* 2012; Schofield & Jolley 2013), further enhances the importance of well constrained index wells in these frontier regions.

The Chevron-operated wildcat exploration well 217/15-1 and sidetrack 217/15-1Z, referred to in the rest of this publication as the Lagavulin well, was drilled in 2010/2011 within the UK sector of the northern Faroe-Shetland Basin (FSB) approximately 200 km north of the Shetland Islands (Fig. 1). The well penetrated a little over 2.6 km of volcanic stratigraphy making it one of the thickest offshore drilled sections through volcanic rocks of the NAIP to date (Fig. 1).

The well therefore provides a unique opportunity to investigate the volcanic development of the NAIP in a previously unexplored area ~100 km NE of the nearest well within the FSB (214/4-1). The importance of the well section lies both in constraining regional stratigraphy in a basin analysis context (Naylor *et al.* 1999; Mudge & Jones 2004; Schofield & Jolley 2013; Austin *et al.* 2014) as well as in terms of the evolution of the NAIP as a whole. This paper utilizes integrated geophysical, petrophysical, lithological, geochemical and mineralogical data for the volcanic rocks from the Lagavulin well to develop a stratigraphic and petrogenetic model for the emplacement of the penetrated volcanic rocks.

Age of the sequence

The composition of the palynoflora throughout the Lagavulin well section is of latest Palaeocene to earliest Eocene character. Occurrences of *Caryapollenites* including *C.*

circulus (3426 m, 4444 m and 4642 m) in association with common *Alnipollenites verus* in both the upper and lower sub-aqueous sequences are important. Specimens of *Caryapollenties circulus* are not recorded in-situ in the Faroe-Shetland Basin in sedimentary rocks older than the base of Sequence T40 (Ebdon *et al.* 1995). Common occurrences of *Alnipollenites verus* (pollen of a wetland plant related to modern Alder) are recorded in the Faroe – Shetland Basin throughout the upper part of Sequence T40, a regional response to the greenhouse climate of the PETM. Occurrences of these taxa therefore indicate that the whole of the Lagavulin section examined in this study is attributable to Sequence T40 (Jolley 2009).

Significant reworking at the base of the well penetration is demonstrated by the wide age range of mixed rare dynocysts, spores and pollen derived from Jurassic to Late Palaeocene strata. Co-occurrences of rare Late Palaeocene marine dynocysts including *Alisocysta margarita* (extinction at top Sequecne T38) and *Palaeocystodinum bulliforme* (T22-T28 equivalent), *Spiniferites 'polygonalis'* and momrphotypes of *Areoligera cf senonensis* (T32-36 equivalent) were documented over intervals of peak reworking, particularly below 4617 m. These mixed age assemblages were recorded in association with the pollen flora noted above and with common freshwater green algae (*Botryococcus braunii*) and acanthomorph acritarchs. Records of these mid to outer shelf normal salinity marine dynocysts are incompatible with the more common algae suggesting that the Palaeocene dinocysts were reworked with the Mesozoic palynofloras as part of the same erosion event.

Methods

Collection of core samples in offshore commercial exploration wells is not a routine procedure due to high operational costs. Consequently, no cores were collected from the Lagavulin well and drill cuttings provide the only means of accessing lithological information about the penetrated formation. 'Ditch cuttings' represent rock fragments returned to the drill floor by the drilling mud along with its component additives. Cuttings are routinely collected and described at the well-head in real time. Drill cuttings vary enormously in their quality, quantity and depth-accuracy depending on a range of factors (Millett *et al.* 2014). Ditch cuttings for the Lagavulin Well were taken every 10 feet (10 feet = 3.048 m) giving approximately 900 individual ditch cuttings samples from the top of the volcanic interval to TD (terminal depth). Unwashed ditch cuttings, i.e. material that included drilling mud and additives, were prepared, screened and analysed using the methodology outlined by Millett *et al.* (2014).

During drilling, down-hole logging tools were deployed supplying near-continuous data on the physical properties of the penetrated formation. Log data including gamma ray (GR), sonic (DTC), neutron porosity (NPHI), density and resistivity are utilized in this study. Some problems were encountered during the collection of wireline log data for Lagavulin with some intervals missing one or more log track acquisitions (Fig. 2 columns D to G). However, for the majority of the penetrated section clear wireline variations are observable. Of particular importance in volcanic facies assessment are the sonic log (DTC), gamma-ray log (GR) and resistivity logs, all of which have near complete well coverage (Fig. 2). Log profiles along with interval velocity histogram analysis have been undertaken for the Lagavulin data (e.g. Nelson *et al.* 2009a & b).

For about 75% of the formation (c. 680 samples) washed ditch cuttings contained fragments of rock at the millimetre scale, which allowed straightforward examination and classification using a binocular microscope. For 100 samples with clear volcanic textures and mineralogy, 20-30 g of volcanic rock chips were individually hand-picked for geochemical analysis. Samples were selected on the basis of the availability of sufficient representative rock material. Bulk-rock material was analysed by X-ray Fluorescence Spectrometry at the University of Leicester (supplementary data). Additional Electron Microprobe Analysis (EMPA) was undertaken on glass and phenocrysts from selected intervals at the University of Aberdeen (supplementary data).

Ditch cuttings

The quality and accuracy of ditch cuttings produced by drilling can be highly variable depending primarily on the type of drill bit employed and the efficiency of drilling fluid circulation. Large thicknesses of the Lagavulin well encountered no or limited drilling problems and consequently yielded exceptionally high quality samples e.g. 50 to 500 g of fragmented rock mostly within the 0.2 – 5 mm diameter range. In the upper parts of the well (~2500 to 3500 m depth) problems related to drilling fluid losses, the phenomenon where drilling fluid escapes into permeable formation, were encountered. At worst this caused no returns whereby no material made it to the rig floor for sampling. In lesser cases contamination with LCM (lost circulation materials added to the drilling fluid to stem losses) and greater mixing of cuttings from different depths occurs. The use of a hybrid drill bit (one incorporating both rock-roller and polycrystalline diamond [PDC] bit technology) over the interval 2375 to 2635 m pulverised the ditch cuttings to a fine powder which accumulated in sheered clumps or rounded cuttings resembling volcaniclastic silt or mudstone. This process produced cuttings which by binocular microscope analysis maintain almost no vestige of their original crystalline nature (Fig. 3b). Only through the identification of fresh olivine fragments (Fig. 3b) by SEM (scanning electron microscopy), and the presence of diagnostic wireline signatures, was the lava flow dominated nature of this interval identified. After this depth conventional rock roller drill bits were employed, which produced good quality cuttings for most of the remainder of the well. Additional issues with cuttings samples occurred at depths > 4500 m where poorly consolidated formation was eroded by drilling and drilling fluid circulation (‘washouts’). Larger rock fragments of >5 mm were dismissed as out-of-sequence (‘cavings’) from uncased borehole sections. The effect of wash-outs and cavings is to create mixed assemblages of cuttings not derived exclusively from the cutters at the recorded depth of penetration.

The analyses of cuttings from the Lagavulin well using the ternary classification scheme of Millett *et al.* (2014) are summarised in Figures 2 and 3. Intervals where cuttings data are deemed to be affected significantly by drilling-related issues have been highlighted on the compiled cuttings log (column C in Fig. 2) and the inference from cuttings treated with due care. From this analysis, significant and systematic variations in the type and abundance of diagnostic ditch cuttings through the well have been identified (Fig. 2 columns A & B). The entire range of ternary end members (see Millett *et al.* 2014 for classification) from crystalline / scoriaceous-dominated, through volcanic glass-dominated, to epiclastic-dominated sequences are represented within the well, as well as a range of percentage mixtures of each end-member. The type and relative abundances of the various cuttings populations has allowed the interpretation of specific intervals of coherent volcanic facies. For extrusive volcanic rocks, which make up the majority of the penetrated section, four principal facies associations are recognized; i) tabular flows; ii) compound pahoehoe flows or flow-fields; iii) hyaloclastite and hyaloclastite breccia and iv) volcaniclastic rocks (Fig. 2 column H). Selected examples displaying features not obvious from the percentage logs alone are presented in Figures 3 and 4 and discussed below.

From ~4080 m downwards large percentages (>90 % in a number of intervals) of densely olivine-phyric crystalline followed by glassy to altered cuttings become common. In some cases >50 % olivine phenocrysts are observed with many containing small euhedral chrome spinel and lesser melt inclusions (Fig. 3e). Dendritic intergrowths of pyroxene and plagioclase identified by the SEM confirm the quenched origin of the glassy cuttings, similar to those reported from sub-marine basalts (Bryan 1972). This lower sequence of glassy cuttings differ from those in the upper hyaloclastite sequence (Fig. 2). The upper hyaloclastite sequence is dominated by cuttings of composite angular glass shards whereas the cuttings from the lower sequence are predominantly present as individual fragments suggesting greater alteration, poorer consolidation or larger average clast size in the lower sequence. The glass shards in the upper sequence comprise sideromelane basaltic glass where fresh and concentrically zoned palagonite where altered. Fresh olivine, clinopyroxene and plagioclase micro-phenocrysts are observed in fresh sideromelane shard cores (Figs 3g & h).

In the lowermost 500 m of the well (~4800-4300 m) ditch cuttings of mixed volcanic origin displayed significant rounding in some cases (Fig. 3c). In many cases these cuttings were composed of hard olivine phyric basalt and glass. Abrasion of hard cuttings by drill bits generates crushed or angular cuttings whereas transport by fluid circulation up the annulus only has the potential to round very soft clay / silt derived cuttings. The presence of these very well rounded hard volcanic cuttings is therefore interpreted to be a primary function of mechanical reworking prior to or during original deposition. This evidence is used to infer significant amounts of reworking of primary volcanic particles either by wave or fluvial action within the interval.

Over the lowermost ~ 300 m of the Lagavulin well a significant percentage (up to ~50 %) of the crystalline cuttings comprise leucocratic medium crystalline material (Fig. 3d). SEM analysis of these cuttings identified that they comprise dominantly basaltic components in the order of abundance plagioclase feldspar >> clinopyroxene > ilmenite needles. No features which may have inferred an extrusive origin such as vesicles or variations in alteration have been observed from these lower cuttings and therefore an intrusive origin is currently preferred.

Wireline logs

The petrophysical properties and associated wireline responses of key volcanic facies from various volcanic settings have been investigated in detail over the past few decades (Planke 1994; Planke & Cambray 1998; Helm-Clark *et al.* 2004; Bartetzko *et al.* 2005; Nelson *et al.* 2009a; Watton *et al.* 2014a). From these and other studies, a relatively high level of confidence in volcanic facies assignation from well data may be achieved in many cases. These include the main facies building blocks of LIPs; simple tabular lavas, compound braided lavas, hyaloclastites, intrusions and interbeds (Jerram 2002; Nelson *et al.* 2009a).

Figure 4 displays results from wireline log analysis including interval velocity histograms for selected key packages of the volcanic stratigraphy, along with annotated representative log profile responses from within each package. The velocity histogram fields from Nelson *et al.* (2009a) have been superimposed beneath the relevant inferred facies type to allow comparison with known velocity responses from boreholes on the Faroe Islands. The interpreted classic tabular flow facies show clear similarities with published wireline profiles (Planke 1994) and velocity histograms (Nelson *et al.* 2009a) allowing confidence in the facies association whilst corroborating inference from cuttings (Millett *et al.* 2014). Within this section around 20 lavas can be identified by their diagnostic asymmetric log profiles (Planke 1994) ranging in thickness from 6 to 40 m (average 16 m). The Beinisvørð Formation penetrated within the Lopra 1 borehole on the Faroe Islands displays similar facies at a slightly higher average thickness of 20 m (Hald and Waagstein 1984).

The interval defined as compound-braided lava facies also shows good agreement with the wireline responses from the Glyvursnes-1 borehole on the Faroe Islands (Japsen *et al.* 2005; Nelson *et al.* 2009a) but with a slightly more restricted velocity range (Fig. 4). Instead of the double-peaked distribution recorded by Nelson *et al.* (2009a), the Lagavulin data comprise a single peak within the middle of the Glyvursnes-1 distribution. The narrower array within the Lagavulin data may relate either to thinner flow cores and / or greater degrees of alteration, a process which is known to decrease the velocity of basaltic rocks (Planke *et al.* 1999a). Cuttings comprising highly amygdaloidal variably altered crystalline basalt (Fig. 4) over this interval gives strong evidence to support a compound-braided facies origin (Millett *et al.* 2014).

The interval defined as hyaloclastite (Fig. 4) comprises a very uniform log character sequence with an almost identical velocity histogram to the hyaloclastite sequence from the Lopra-1/1A well (Nelson *et al.* 2009a). Intervals of lower velocity and resistivity may represent intervals of increased reworking, alteration, differing grain size or higher porosity within the sequence; all features well documented from field (Watton *et al.* 2013; Frolova 2010) and borehole examples (Andersen *et al.* 2009; Watton *et al.* 2014b) from Iceland, the FSB and Hawaii. No cuttings were available for comparison over the lower part of this hyaloclastite section (from ~3310 m) due to lost returns (Figs 2 & 4). The inference from cuttings before the loss of returns suggest a very uniform character of hyaloclastite (Fig. 4).

The interval between 4100-4430 m depth, excluding a thin interval of lavas between 4133-4235 m, comprises a much more heterogeneous sequence than the previously discussed intervals with a wide ranging velocity histogram (Fig. 4). The uniformly low gamma response suggests that the sequence is dominated by low GR basaltic material. The heterogeneity suggests that the sequence comprises highly variable physical properties but also that these variations are not generally systematic as for instance is observed in the simple tabular lavas. A number of features within the sequence are used to constrain its volcanic facies origin. Firstly, a significant peak in high velocity measurements (c. 6.5 km/s) are recorded over the interval, these being higher than the lava cores of the classic tabular flows (c. 5.8 km/s) from higher in the sequence. Olivine phenocrysts have previously been demonstrated to increase the average velocity of Hawaiian basalt (Manghnani & Woollard 1965) and hyaloclastites from the Hawaiian Scientific Drilling Program borehole (Watton *et al.* 2014b). We therefore envisage a similar explanation for this sequence of the Lagavulin well which includes abundant high Mg olivine.

The facies is hard to infer from the wireline responses alone. It is plausible that a number of the high velocity intervals (Fig. 4) may represent lavas but they may as easily represent coherent flow lobes within a hyaloclastite delta sequence (Skilling 2002). The heterogeneous log responses in the upper half of the section (Fig. 3) can only be reconciled with highly variable formation including coherent high velocity blocks or bodies intimately associated with much finer grained and / or altered volcanic material. From the wireline logs we interpret the section to comprise a hyaloclastite / breccia sequence including coherent flow lobes. The abundance of densely olivine phyric glass along with a very mixed and altered overall assemblage supports this type of scenario.

Possible intrusions were identified from the presence of fresh coarser grained crystalline cuttings. The example presented in Figure 4 displays log responses through a potential intruded section at 3830-3850 m depth. The interval shows very low and uniform GR counts below the already low background values of the lavas, a feature identified by Boldreel (2006) from dolerite intrusions into lavas in the Lopra-1/1A borehole. The interval also displays slightly elevated velocity and resistivity and overlaps with the velocity histogram for dolerite intrusions encountered in the Lopra-1/1A well (Nelson *et al.* 2009a). The box shape profile typically seen for intrusions into sediments (Planke *et al.* 1999b) is not present nor expected due to the much diminished difference in velocity between lavas and an inferred dolerite intrusion. The chemistry of the samples (discussed later) shows little to no deviation from the background lavas aside from lower LOI and slightly elevated Mg# which neither supports nor contradicts an intrusive origin.

The lowermost section of the Lagavulin well (4430-4865 m) comprises similarly heterogeneous wireline log responses to those of the overlying olivine hyaloclastite / breccia sequence but at noticeably decreased maximum velocity (see Fig. 2). A number of high GR units are present over this interval interdigitated with low GR background basalt levels down to TD at 4865 m. Silt grade siliciclastic material was also recorded at the well site over some of the high GR intervals also supporting the presence of increased levels of non-volcanic material in the lower parts of the well. The slightly raised but still low background GR levels may be explained by high levels of alteration (Planke *et al.* 1999a) of a basaltic dominated volcaniclastic sequence along with minor non-volcanic mixed components as suggested by the altered mixed volcanic cuttings data over the interval. The significant evidence for reworking of volcanic grains (Fig. 3c) identified from cuttings also supports this scenario.

Leucocratic dolerite cuttings were encountered at the base of the well after the majority of the log data (aside from resistivity and GR) ends precluding attempts to identify associated petrophysical signatures. A high resistivity interval (4755-4805 m) with uniform moderate GR could hypothetically represent a more evolved intrusion (Delpino and Bermúdez 2009) but without velocity data it is not possible to explore this further.

Seismic Data

The lithostratigraphic scheme derived from the above analysis (Fig. 2 column H) includes facies and facies transitions that comprise distinctive differences in velocity and density. These variations should therefore display differences in seismic data. Figure 5 displays a seismic line across Lagavulin with the well facies scheme superimposed. The data forms part of PGS's Corona Ridge Regional Geostreamer 2D survey, which was specifically acquired and processed to improve imaging through the volcanic pile.

From the data it is clear that many of the main transitions and facies packages show distinct accompanying seismic responses. Of key interest are the clear transitions between lavas and hyaloclastite packages and the identification of the significant hiatus-related interbed horizon. This hiatus therefore implies the possibility of inter-lava sediment accumulations at this time period elsewhere in the basin where accommodation space and sediment catchments were more favourable (Schofield & Jolley 2013; Ebinghaus *et al.* 2014).

The interpreted hyaloclastite packages display weak traces of foreset morphologies similar to those seen in other hyaloclastite deltas within the FSB (Wright *et al.* 2012). Lateral discontinuities and internal heterogeneity within the interpreted packages suggest a potentially complex 3D facies architecture (Watton *et al.* 2013). Interestingly the packages appear to thin in opposite directions suggesting that they may have been fed from different directions. Tracking these horizons through the seismic survey and potentially more regionally is out with the scope of this contribution and will comprise part of a future research program. Possibilities that may be investigated in future work include changes in eruption fissure locations, reorganisation of the lava drainage system and palaeogeographic modifications to accommodation space during the evolution of the volcanic pile.

Geochemistry

Geochemical sample intervals were predominantly in the range of 40-90' (~12-30 m) with exceptions occurring where drilling fluid additive contamination, lost returns or sample availability rendered sampling impossible or useless. Lesser coverage in the lowermost section of the well is a consequence of the high levels of mixing and cavings. Thirteen packages of volcanic stratigraphy comprising flow or flow groups have been recognized (Figs 6 & 9) based on geochemical considerations alone, without recourse to wireline logs or cuttings analysis. A flow or flow group was defined as two or more consecutive sampling points that exhibited similar chemical signatures. A new group was selected where adjacent samples displayed systematic chemical variations significantly greater than the analytical precision of the method (supplementary data).

Loss on ignition (LOI) at 750°C is up to 8.0 weight % for some of the most altered samples and so the possibility of post-emplacement mobility of major elements in these cases is significant (Fig. 6). For compositions with Mg# > 60 there is a broadly positive correlation between Mg# and LOI. Since samples with Mg# > 70 are predominantly from hyaloclastite sequences, high LOI is most likely to be the result of hydration of glass during and/or after emplacement. Samples with Mg# in the range 45-70 mostly have LOI < 4 weight % which are considered here to be acceptable levels for basaltic rocks. Volcanic unit VI has LOI of 5-7 weight % and Mg# 34-40. This unit comprises highly weathered compound pahoehoe flows with abundant amygdales and also contains substantial red bole development. Subaerial weathering of basalt follows predictable patterns of depletion and enrichment in major element oxides, and there are a number of chemical indexes that can be used to characterize such weathering profiles (e.g. Maynard 1992; Nesbitt & Wilson 1992; Babechuk *et al.* 2014). Here, the magnesium index (MgI; molar $Al_2O_3/(Al_2O_3 + MgO)$ x100) of Maynard (1992) has been used to monitor post-emplacement mobility of major element oxides. MgI for fresh volcanic rocks varies from < 10 for picrites (Mg# > 70) up to c. 50 for basalts with Mg# of

40-60 (Fig. 7). During weathering the greater mobility of MgO compared to Al_2O_3 and iron oxides causes MgI to increase and Mg# to decrease with increasing intensity of weathering (Fig. 7). Volcanic unit VI has both the lowest Mg# (34-44) and highest MgI (57.5-66.5) of any of the volcanic units investigated, and exhibits similar geochemical patterns of elemental enrichment and depletion to those reported for weathering profiles of basalts from the Deccan Traps and South Australia (Nesbitt & Wilson 1992; Babechuk *et al.* 2014). The remainder of the Lagavulin samples do not exhibit any evidence of significant major element mobility in terms of correlations between MgI and Mg#. Samples with Mg# > 70 and LOI up to 8 weight % overlap with the composition of unweathered picrites from Baffin Island in terms of MgI and Mg# (Fig. 7) implying that hydration of glass was not necessarily accompanied by significant loss of major elements.

Major elements recalculated to 100% on a dry basis are plotted versus Mg-number (Mg#) in Figure 6 (additional plots in supplementary data). Mg# varies from 35-85 but samples with Mg# <40 are exclusively from weathered volcanic unit VI. All the samples with Mg# > 70 are from volcanic units I and III and comprise glassy cuttings containing Mg-rich olivine (Fo_{85-90}) ± diopsidic augite ($En_{39}Wo_{47}Fs_{14}$) ± labradorite (An_{77-80}). Elevated Cr and Ni abundances (up to 2900 and 1600 ppm respectively; Fig. 8) indicate accumulation of olivine ± Cr-spinel and probably augite in these samples. For the remaining samples major element data are rather scattered, likely contributed to by alteration and the ditch cuttings nature of the samples. However, some clear systematic variation is seen in the data. SiO_2 exhibits a positive correlation with Mg#, whereas for Fe_2O_3, TiO_2 and P_2O_5 data fall into two main clusters which overlap at Mg# c. 52. Samples with Mg# > 50, TiO_2 < 1.5, P_2O_5 < 0.15 and Fe_2O_3 < 13.5 weight % predominate in the lower parts of the stratigraphy, whereas samples with Mg# < 50, TiO_2 > 1.5, P_2O_5 > 0.15 and Fe_2O_3 up to 15.7 weight % predominate in the upper part of the stratigraphy (Fig. 9). Electron microprobe analyses of glass from volcanic unit VII form an extension of the high TiO_2, P_2O_5 and Fe_2O_3 arrays seen in whole rock cuttings samples from the upper part of the stratigraphy. Correlation between Mg# and CaO is positive for Mg# <55 and negative for Mg# >55, a consequence of early olivine and later augite-dominated fractionation. The leucocratic low TiO_2 c. 1 wt. % dolerite sample from the base of the well (15,750') displays the highest SiO_2 c. 52 wt. % of the well with low CaO c. 8.6 wt. % and high K_2O c. 1.3 wt. % relative to other samples of the LTZ suite at similar Mg#. This along with higher than average Ba/Zr of 2.7 suggests possible modification by crustal contamination (Fitton *et al.* 1998). Compositions (e.g. dacites) recording evidence for significant assimilation of crustal components are observed at the base of a number of other well penetrations in the NAIP margins including on the Rockall Trough, Vøring margin and the Erland volcano (e.g. Morton *et al.* 1988; Viereck *et al.* 1989; Kanaris-Sotiriou *et al.* 1993) and within the Middle Series of ODP Leg 152, SE Greenland Margin (Fitton *et al.* 1998). The Lagavulin well may therefore have penetrated rocks representing a much less advanced stage of this regionally important process.

Zr abundances vary from 23 to 233 ppm for the suite as a whole with Ti/Zr (c. 100) and P/Zr (c. 6.0) being consistent across the entire range of major element compositions. However, two lineages of samples are evident on plots of Y and Nb versus Zr (Fig. 8) one forming a cluster around Zr/Y = 2.5 and Nb/Zr <0.03 and the other at Zr/Y = 5.0 and Nb/Zr c. 0.08. Samples from volcanic units I and III scatter about Zr/Y = 2.5 and have Zr < 50 ppm and Y <15 ppm, which considered along with Ni > 600 ppm and Cr > 1000 ppm is a predictable consequence of the accumulation of olivine plus Cr-spinel in these samples. Samples with Zr/Y c. 5.0 all contain > 1.5 weight % TiO_2 and those with Zr/Y c. 2.5 contain ≤ 1.5 weight % TiO_2. Scatter of Sr and Ba concentrations is a likely effect of alteration combined with minor barite drilling mud contamination of the samples (supplementary data). Notwithstanding the ditch cutting sample material and alteration of some samples, it is clear that there are two distinctly recognizable lineages of volcanic rocks in the Lagavulin well.

For the purposes of further discussion these will be referred to as high TiO_2 and Zr (HTZ) and low TiO_2 and Zr (LTZ) types. Volcanic unit VI has TiO_2 c. 1.5 and Zr/Y c. 3.7 plotting partly between LTZ and HTZ, and Nb/Zr c. 0.03 consistent with and LTZ affinity. Given the evidence for extended subaerial exposure and weathering in unit VI we consider it a member of the LTZ suite whose major element characteristics have been modified. Zr, Y and Nb are immobile during pedogenesis and low grade metamorphism of basalts (e.g. Babechuk *et al.* 2014; Morrison 1978). Consequently, no systematic variation in Zr/Y or Nb/Y with increasing LOI is observed within either the LTZ or HTZ group data enabling their use as petrogenetic indicators for unit VI samples. Including unit VI, the lower 1,300 m of the well is almost exclusively of the LTZ type, with a single excursion to HTZ type in unit II (Fig. 9) over a depth range of 4142-4166 m. It may be that these originate from minor intrusions within this section although no clear log signatures confirm an intrusive origin. In the depth interval 2721-3511m, HTZ volcanic rocks predominate with an excursion to LTZ at volcanic units VIII and X at 3093 and 2910 m respectively. Samples are sparse above 2682 m but available data suggest a return to LTZ compositions above this depth.

Discussion

Stratigraphic development of the volcanic succession.

Figure 11 summarises the interpreted stratigraphic development of the volcanic succession encountered in the Lagavulin well. Integration of ditch cuttings, wireline logs and seismic data has enabled the identification of distinct and genetically important volcanic facies variations through the well with a high degree in confidence.

The bottom ~600 m of the succession comprises lithofacies packages that are consistent with the progradation of a hyaloclastite delta into standing water. Reworked pro-delta facies are inter-fingered with mixed lithologies including epiclastic mud and silt and are capped by hyaloclastite. The hyaloclastite is in turn overlain by a thick sequence of lavas representing the emergence of the lava pile. Similar progressions are seen onshore in many places including East Greenland (Pedersen *et al.* 1997), James Ross Island, Antarctica (Skilling 2002) and the Columbia River Basalt Province (Fig. 10) and have been clearly imaged in sub-surface seismic sections in the FSB (Wright *et al.* 2012).

After a period of emergence which allowed time for significant weathering of the subaerial lava surface, the lava pile became submerged and a new hyaloclastite delta system developed. Once this second lava delta became emergent, thick tabular lava flows developed on its surface, and volcaniclastic and epiclastic debris accumulated on top of the subaerial lava flows in locally developed drainage systems.

A mixed volcaniclastic/epiclastic succession dominates the top of the volcanic sequence (2590-2200 m) indicative of a period where no lavas or hyaloclastite were deposited in-situ at the Lagavulin site. Instead, sediment derived from erosion of emergent parts of the volcanic landscape accumulated at the Lagavulin site before a final large lava flow erupted signalling the end of the eruptive history.

Relative base-level changes

The occurrence of thick sequences of hydro-volcanic and sub-aerial volcanic rocks within the well indicates that the availability of water at the site varied considerably during volcanism. Palaeo-environments have been designated as 'sub-aerial' conditions where subaerial lava flows are dominant, 'submerged' where hyaloclastite, hyaloclastite breccia or epiclastic sediments are dominant, and 'standing water' where minor volcanic glass and or epiclastic sediment excursions occur (Fig. 10). Major transitions from submerged to subaerial sequences at depths ~4100 m and ~3125 m may indicate lava delta progradation followed by sub-aerial aggradation, relative uplift or a combination of these processes. Significant reworking identified from both ditch cuttings and bio-stratigraphic analysis towards the base of the Lagavulin well suggest that significant basin flank uplift occurred prior to eruption of the oldest preserved Lagavulin strata.

In contrast, the sudden change from deeply weathered subaerial lavas with interbedded reddened soils and volcaniclastic units to hyaloclastite at 3520 m depth documents a re-submergence of the volcanic pile at this time. Consequently, the volcanic successions above and below the top of unit VI (Fig. 10), both exhibit internal features consistent with the stratigraphic development of lava deltas; however, the change from subaerial lavas to hyaloclastite between units VI and VII does not, and suggests an external control i.e. changing relative water level.

The ~975 m stratigraphic thickness between these two emergence points (~4100 m and ~3125 m) therefore requires a relative base level change at this time. The upper mixed volcaniclastic / epiclastic succession (2590-2200 m) may also represent further relative subsidence but given the lack of evidence for in-situ hydro-volcanism, local reworking and accumulation of sediment by surface drainage of the lava field may also have contributed to this sequence (e.g. Hole *et al.* 2013).

A number of studies have identified evidence for rapid uplift and subsidence events within the FSB (Ebdon *et al.* 1995; Nadin *et al.* 1997; Shaw Champion *et al.* 2008; Hartley *et al.* 2011) and the broader NAIP (Saunders *et al.* 2007) based on backstripping subsidence histories and seismic mapping of Palaeocene to Eocene aged sequences. Thermal effects and volcanism associated with the proto-Iceland plume along with pre-, syn- and post Palaeocene rifting within or nearby to the basin all contribute to its complex stratigraphic history. Hartley *et al.* (2011) for instance record three phases of ~200-400 m uplift in the Judd sub-basin with maximum uplift peaking at ~55.5 Myr followed by rapid subsidence causing flooding of the associated unconformity surface within ~3 Myr of the onset of uplift (Shaw Champion *et al.* 2008). Relative base level changes are also identified from the offshore volcanic sequences associated with lava delta development (Wright *et al.* 2012) and mixed volcanic and sedimentary sequences (Schofield & Jolley 2013). Similarly, flooding events are identified within the sub-aerial dominated onshore Faroe Islands Basalt Group (FIBG) including intra-T40 Lower Flett Formation equivalent events which have been correlated with large scale magmatic cycles (Jolley *et al.* 2012) and which can be correlated to the offshore FSB sequences (Passey & Jolley 2009; Schofield & Jolley 2013).

The magnitude and timing of transient uplift recorded in the Judd basin is concluded by Shaw Champion *et al.* (2008) not to be consistent with either conductive cooling of hot mantle beneath the region or with changes in global sea level during this period. Instead, a transient pulse or pulses (Hartley *et al.* 2011) of buoyant hot material spreading radially by convection beneath the region away from the proto-Iceland plume has been proposed to account for transient uplift events. Depth dependent thinning of the lithosphere during failed Palaeocene rifting of the FSB has also been proposed to explain excess post Palaeocene subsidence (Fletcher *et al.* 2013). The volcanic facies of the Lagavulin well records eruption development consistent with transient uplift during T40 lower Flett Formation times suggesting development prior to the major T40-T45 sequence boundary of Ebdon *et al.* (1995).

Estimating the amount of tectonic subsidence recorded at the Lagavulin site is not simple due to the volcanic nature of the depositional system and facies along with a lack of knowledge about the sub-basalt stratigraphy. Different rates of alteration, secondary mineralisation and burial compaction all complicate the already wide range of initial rock strengths known for different volcanic facies precluding a straightforward method of backstripping the mixed volcanic sequence. We restrict our current study to a simple estimate of the loading effect of the ~975 m volcanic package (separating the emergence intervals at ~4100 m and ~3125 m) by assuming simple local 1D Airy isostasy. Using the assumptions outlined in the supplementary data, a rough minimum value of ~334 m tectonic subsidence (total minus isostatic) is estimated. Non-instant compensation, lithospheric flexure and the occurrence of tectonic uplift during deposition of the sub-aerial sequence would all serve to increase the tectonic subsidence component for this interval whilst syn-eruptive delta subsidence (Wright *et al.* 2012) would have the opposite effect. This will be further investigated in future work but initially, tectonic subsidence on the order of at least a few 100's of meters is inferred at the transition between LTZ to HTZ compositions.

A similar lava delta development sequence is recorded from seismic and well data (214/4-1) to the south of Lagavulin (e.g. Wright *et al.* 2012; Passey 2004). A large prograding T40 Lower Flett Formation (Schofield & Jolley 2013) delta system equivalent to the Beinisvørð Formation (Passey & Jolley 2009; Wright *et al.* 2012) of the FIBG is recorded prior to inferred initial subsidence of ~200 m. It therefore appears possible that the main 214/4-1 emergent delta and the Lagavulin lower LTZ delta may record broadly equivalent histories.

Petrogenesis

The pseudo-ternary system Diopside-Enstatite-Anorthite can be used to estimate final pressure of equilibration of Si-saturated tholeiitic basalts (equation 6 of Herzberg 2004) and for Units I-IV estimates are ~0.5±0.3 GPa. Units VII-XI equilibrated at near 0 GPa, although around 50% of samples are Ne-normative and Si-under-saturated and cannot yield pressure information. The low pressure of equilibration is in contrast to the major plateau forming lavas of the BPIP most of which equilibrated at ~0.9 GPa (Thompson 1982). Three LTZ samples from Lagavulin provide PRIMELT3 solutions for primary magmas (Herzberg & Asimow 2015; Hole 2015). One sample from unit I (14300') and two from Unit IV (13370' and 13430') indicate potential temperatures of T_P~1530°C with initial intersection of the dry peridotite solidus at ~4.1 GPa (supplementary data). Olivine equilibration temperatures on samples from the same units, calculated using the method of Putirka *et al.* (2007), independently indicate ~1450°C at 0 GPa, which is coincident with the adiabatic pressure-temperature melting curve for T_P~1550°C. These T_P estimates are similar to those obtained for 60-61 Ma Baffin Island picrites (Hole 2015) indicating that melting beneath Lagavulin required a significant thermal anomaly of ambient T_P +180-200°C. However, the extent of melting was for the Lagavulin samples (F=0.13-0.18) considerably lower than that for Baffin Island (F=0.29; Hole 2015), most likely a function of thicker continental lithosphere beneath Lagavulin than at Baffin Island. HTZ samples are more evolved than LTZ samples and do not yield PRIMELT3 primary magma solutions.

The Lagavulin LTZ samples exhibit generally low Zr/Y and Nb/Y ratios that overlap with those for N-type MORB, picrites from Baffin Island and basalts from the seaward dipping reflector sequences at Hatton Bank and Rockall Trough (DSDP Leg 81; Fig. 11). The parameter ΔNb (Fitton *et al.* 1997) represents the deviation of a data point above or below the lower bound of the Iceland array such that +ve ΔNb characterizes Icelandic plume source affinity and –ve ΔNb characterizes N-type MORB affinity, (Fig. 11). LTZ basalts also have ΔNb in the range -0.2 to -0.5 which, along with the very low abundances of incompatible trace elements, low Zr/Y and low Nb/Y is consistent with derivation from large degrees of partial melting of a depleted mantle source similar to N-type MORB. Consequently, there are similarities in the petrogenetic histories of Baffin Island low ΔNb picrites both in terms of geochemical compositions and T_P. HTZ samples have higher ΔNb in the range -0.07 to 0.0 and significantly higher Zr/Y and Nb/Y than the LTZ group with compositions overlapping with the high TiO_2 series basalts from the FIBG and Central East Greenland (Søager & Holm

2011). The consistently high Zr/Y c. 5 of the HTZ groups suggests that they represent smaller degrees of partial melting than the LTZ basalts which along with the higher ΔNb suggests a potentially more enriched source. Variations in melting model parameters (Stracke *et al.* 2003) along with isotopic evidence (Waight & Baker 2012) have, however, also been used to argue that ΔNb cannot unequivocally separate Icelandic from MORB source components in all cases. Acknowledging these constraints on the origin of variations in ΔNb, the inter group variations revealed in Figure 10 remain regionally significant because it is difficult to move between e.g. groups V and VII by different degrees or depths of melting of the same source with realistic melting parameters (e.g. Fitton *et al.* 1997; Stracke *et al.* 2003). Inference towards degree of melting based on incompatible element ratios such as Zr/Y may also be complicated where active upwelling beneath a plume head operates (Maclennan *et al.* 2001). However, given the large distance (likely >600 km) of the Lagavulin site to estimates of the plume epicentre beneath central Greenland between 60-50 Ma (e.g. Lawver & Müller 1994), we envisage a passive upwelling scenario in which increasing Zr/Y increases with decreasing melting.

Zr/Y and ΔNb are plotted against stratigraphic height in Figure 11 to indicate extent of melting and possible changes in mantle source respectively. We identify the sudden volcanological and geochemical transition that took place between units VI and VII as a significant change in the mantle melting regime that fed the Lagavulin lava pile at this time. This inferred decrease in extent of melting over such a short timescale may be associated either with decreasing mantle temperatures or with geographically separate melting regions with different lithosphere thicknesses feeding the lava pile at different times.

There is little evidence for major syn-eruptive shallow crustal faulting over the Lagavulin structure (Fig. 5) or in the FSB in general (Fletcher *et al.* 2013). Consequently, if the LTZ magmas were generated locally beneath the area then the lithospheric thinning must either have been pre-magmatic and associated with Cretaceous rifting of the FSB (Doré *et al.* 1999) or depth dependent (Fletcher *et al.* 2013) and related to Late Palaeocene failed rifting of the basin.

We cannot fully rule out at this stage that the LTZ magmas migrated (either as sub-surface intrusions or surface eruptions) laterally from a location of active rifting to the north (e.g. Fletcher *et al.* 2013; Millett 2014; Hole *et al.* 2015). Low TiO_2 sequences are for instance recorded in the syn-breakup successions of the Faroe Islands and East Greenland and are interpreted to represent extensive melting beneath rapidly thinning lithosphere at the onset of major continental rifting between the Faroe Islands and East Greenland (Larsen *et al.* 1999). The low TiO_2 lavas have also been inferred to comprise depleted plume source components based on isotopic evidence (Søager & Holm 2011; Waight & Baker 2012). However, both the current age estimate ~T40 and the relative stratigraphic position of the LTZ magmas (dominating the base of the Lagavulin sequence) appears to argue against an origin equivalent to the low TiO_2 magma suites of the FIBG (T45 Malinstindur and Enni Formations, Passey & Jolley 2009) and age equivalent Central East Greenland successions (Milne Land to Rømer Fjord Formations, Larsen *et al.* 1999; Søager & Holm 2009; Waight & Baker 2012). In both of these cases the low TiO_2 larger degree melts become important towards the top of the respective sequences subsequent to but also coeval with extensive high TiO_2 lavas which overlap in Zr/Y/Nb space with the HTZ Lagavulin lavas (e.g. Fitton *et al.* 1997; Søager & Holm 2009). The main Lagavulin succession appears to correspond to a pre-breakup equivalent sequence (Larsen *et al.* 1999) but showing different chemical development potentially as a function of pre-thinned lithosphere beneath the area.

We are unaware of any other location in the rift-proximal Palaeogene NAIP sequences where there is the stratigraphic record of at least 1.3 km of low TiO_2, low Zr/Y tholeiites being emplaced prior to the major onset of high Zr/Y basalts. Whilst low Zr/Y picrites are well-known from pre-breakup lava successions of West Greenland (e.g. Vaigat Formation; Dale *et al.* 2008; Larsen & Pedersen 2009) these are considered to be older (c. 60.5 Ma, Storey *et al.* 1998) than the Lagavulin sequence. N-MORB type lava compositions are also known from the Erland central volcano to the south of Lagavulin supporting the existence of short lived large degrees of melting beneath the FSB near the Palaeocene-Eocene boundary (Kanaris-Sotiriou *et al.* 1993; Jolley & Bell 2002b). N-MORB affinity compositions are inferred to have mixed with dacitic compositions of the Site 642 Vøring Margin Lower Series (~140 m) prior to eruption of the thicker Upper Series (~760 m) which plots transitional between the LTZ and HTZ Lagavulin compositions (Fig. 11, Viereck *et al.* 1988). Additional geochemical data are required to evaluate in more detail the discussed variations between the Lagavulin well and other NAIP sites and will be presented separately.

The association of LTZ eruption deposits formed by melting of hot depleted mantle and a phase of uplift followed by rapid subsidence in the Lagavulin well appears to potentially fit with a pulsing plume mechanism similar to that proposed by Hartley *et al.,* (2011). In such a case short lived extensive melting may have been promoted beneath the pre-thinned lithosphere of the FSB in the Lagavulin area. Given the T40 age of the Lagavulin sequence, the inferred vertical motions at the site could relate to a number of known relative base level changes in the south of the basin. The eruption of the HTZ lava sequence may represent reduced temperatures coupled with source heterogeneity within the passing plume material. Alternatively they may have been sourced from melting beneath neighbouring areas of thicker lithosphere and travelled laterally to the Lagavulin site. The recurrence of minor LTZ eruptions towards the top of the sequence may simply represent further source compositional heterogeneity or may again relate to differences in eruption locations. Future seismic mapping may identify eruption sites enabling better constraint on these possibilities.

Conclusions

We have presented integrated ditch cuttings, wireline log and geochemical analyses for a ~2.6 km thick sequence of volcanic stratigraphy penetrated north of the Shetland isles. The location and depth of penetration of the Lagavulin well in an unexplored part of the FSB makes it a key stratigraphic and geochemical section for developing understanding of the local and regional NAIP development. This investigation has revealed the following main conclusions.

1. Integrated analysis of data from exploration wells penetrating volcanic successions may be used to compile robust volcano-stratigraphic schemes in large part comparable to scientific coring programs.
2. Volcanic facies analysis of the Lagavulin succession reveals two major submerged to sub-aerial cycles consistent with the development of lava deltas. These sequences are separated by a volcanic hiatus during which time the area became re-submerged recording relative subsidence at this time.
3. Within the age constraints of the well, the base level changes recorded by the volcanic facies appear to correspond to evidence from the SW FSB for transient uplift recorded around the Palaeocene-Eocene boundary.
4. Two major geochemical groups are identified within the well, the first LTZ group was derived from large degree partial melting of a depleted source similar to modern day N-type MORB but potentially comprising a depleted plume component due to high estimated T_p. The second HTZ group was derived from smaller degrees of partial melting of a more enriched source similar to the high TiO_2 lavas found throughout the Faroe Islands Basalt Group and Central East Greenland.

5. A distinct and well constrained change in the dominant geochemistry from LTZ to HTZ compositions occurs at exactly the same level as a volcanic hiatus and relative subsidence event suggesting a genetic link between these features.
6. The association between LTZ compositions, high temperatures e.g. ambient T_P +180-200°C and evidence for a transient phase of uplift may provisionally be related to the passage of hot buoyant plume material beneath the area during T40 times.
7. The dominance of LTZ picrites over the bottom ~1300 m of the Lagavulin succession prior to similar compositions being erupted on the Faroe Islands and Central East Greenland may be reconciled with short lived melting of hot mantle beneath the pre-thinned lithosphere of the FSB in this area.

Acknowledgements

This work was funded by Chevron. The authors would like to acknowledge the Chevron West of Shetlands team along with the Joint Venture partners OMV, Faroe Petroleum and Indemitsu for access to data along with permission to publish this study. PGS are thanked for access to the Corona Ridge Regional Geostreamer (CRRG) data and permission to publish the seismic line. The manuscript was improved thanks to insightful reviews by Stephen M. Jones and Andy Saunders which substantially improved an earlier draft. John Still and Fiona Thompson gave invaluable technical support at the University of Aberdeen and Kieran Wall helped with real-time cuttings analysis.

Figure captions

Fig. 1 Map of the North Atlantic Igneous Province. a) Distribution of the onshore and offshore basaltic sequences and selected ODP/DSDP boreholes after Larsen & Saunders (1998). Selected boreholes encountering volcanic sequences of the NAIP highlighting the drilled volcanic thickness in brackets (Wood *et al.* 1979; Morton & Keene 1984; Morton *et al.* 1988; Planke 1994; Archer *et al.* 2005). b) Map showing the location of the Lagavulin well in the FSB along with the volcanic sequence thickness of selected offshore commercial wells for comparison (Tobermory thickness from Passey 2004). Onshore Faroe Islands boreholes shown for comparison (Passey & Jolley 2009), extent of extrusive and intrusive volcanic rocks after Rateau *et al.* (2013).

Fig. 2. Stratigraphic column through the Lagavulin well. A. Raw end-member percentage results from the ditch cuttings analysis. B. Non-genetic classification scheme from cuttings after Millett *et al.* (2014). D. Gamma ray log. E. Sonic log. F. Density log. G. Resistivity log displaying deep and shallow resistivity. H. Condensed interpreted facies associations and accompanying descriptions. Note: depths are displayed as measured depth (MD), true vertical depth subsea (TVDss) is 105' (~32 m) shallower than MD for the original 217/15-1 hole and increases slightly to 108.37' (~33 m) over the side track 217/15-1Z hole section.

Fig. 3. Examples of key ditch cutting samples. a) Ternary non-genetic classification scheme used for cuttings percentage analysis (Millett *et al.* 2014). b) SEM image of rock flour cuttings including fresh olivine fragments sheared by hybrid drill bit. c) Well-rounded hard olivine phyric cuttings. d) Leucocratic dolerite cuttings from the base of the well. e) SEM image of densely olivine phyric cutting with melt and small chrome spinel inclusions. f) Close up of (e) displaying quench texture dendritic clinopyroxene intergrown with plagioclase and interstitial glass. g) SEM image of hyaloclastite composed of angular sideromelane glass shards displaying concentric alteration to palagonite gel. h) Fresh micro-phenocrysts within sideromelane glass core. Abbreviations, Ol; olivine, Cpx; clinopyroxene, Plag; plagioclase feldspar, Sd; sideromelane.

Fig. 4. Summary of key petrophysical and ditch cuttings responses for the main interpreted volcanic facies. Velocity histograms are generated from sonic log data for key facies intervals with a bin size of 0.1 km/s and compared to the histogram arrays from other NAIP boreholes (Nelson *et al.* 2009a, counts axis manually stretched to current study for comparison). Typical wireline profiles are presented and annotated to display key volcanic features.

Fig. 5. a) NW-SE seismic line across the Lagavulin well showing the interpreted lithology log (see Fig. 1 for location). b) Interpreted seismic line showing the lateral extension of the main volcanic facies. Data courtesy of PGS (CRRG 2D).

Fig. 6. Major element oxides, loss on ignition (LOI) and magnesium index of alteration (MgI = molar $Al_2O_3/(Al_2O_3+MgO)*100$) of Maynard (1992) *versus* Mg-number for volcanic units. The grey triangles are 58 electron microprobe analyses of glasses from unit VII at depths 11140', 11250', 11380' and 11480' (3395, 3428, 3468 and 3499 m respectively).

Fig. 7. MgI *versus* Mg# for Lagavulin samples and weathering profiles developed above lavas at Baynton, Australia (Nesbitt & Wilson 1992) and Chhindwara, Deccan Province (Babechuk *et al.* 2014). MgI assumes that Al_2O_3 is immobile during weathering whereas

MgO is mobile, such that decreasing Mg# with increasing MgI indicates increasing weathering.

Fig. 8. Trace elements (ppm) and TiO_2, and P_2O_5 (both weight %) *versus* Zr (ppm) for basalts with ≤1.5 weight % TiO_2 (open symbols) and those with >1.5 weight % TiO_2 (filled symbols). Shaded areas are the range of compositions of mid Atlantic Ridge basalts from 57-61°N (Murton *et al.* 2002), out with the influence of the Iceland plume.

Fig. 9. Geochemical variations with depth in the Lagavulin well. The grey shaded areas are dominated by high TiO_2 (≥ 1.5 weight %), high Zr (≥ 150 ppm) compositions. ΔNb calculated according to the scheme of Fitton *et al.* (1997).

Fig. 10. a) Log showing Zr/Y, ΔNb, inferred relative water-level and lithofacies distribution *versus* depth. b) Schematic cartoon illustrating development of the lava deltas. The lower cartoon shows the development up to volcanic unit VI at which stage there was a hiatus in volcanic activity. The upper cartoon shows the development of the upper delta sequence with the change in Zr/Y ratio of lavas shown schematically on the left. c) Field example of a small dissected emergent lava delta from the Columbia River Basalt Province, USA, annotated after Skilling (2002).

Fig. 11. Nb/Y *versus* Zr/Y for volcanic units from a) the Lagavulin well, and b) volcanic rocks from the NAIP. Fields for DSDP Leg 81 (Hatton Bank/Rockall Trough) Brodie & Fitton (1998); Faroe Islands, Søager & Holm (2011) and Gariepy *et al.* (1983); IJDS – Islay-Jura regional dyke swarm of the BPIP Hole *et al.* (2015); Mull Plateau Lava Formation (MPLF) Kerr *et al.* (1999); Vøring Plateau, Parson *et al.* (1989) and Viereck *et al.* (1989).

References

Andersen, M.S., Boldreel, L.O. & SeiFaBa Group. 2009. Log responses in basalt successions in 8 wells from the Faroe-Shetland Channel – a classification scheme for interpretation of geophysical logs and case studies. *In:* Varming, T. & Ziska, H. (eds) *Faroe Islands Exploration Conference: Proceedings of the 2nd Conference. Annales Societatis Scientiarum Færoensis, Supplementum,* **50**, 364–391.

Archer, S.A., Bergman, S.C., Illiffe, J., Murphy, C.M. & Thorton, M. 2005. Palaeogene igneous rocks reveal new insights into the geodynamic evolution and petroleum potential of the Rockall Trough, NE Atlantic Margin. *Basin Research*, **17**, 171-201.

Austin, J. A., Cannon, S.J.C. & Ellis, D. 2014. Hydrocarbon exploration and exploitation West of Shetlands. *In:* Cannon, S.J.C. & Ellis, D. (eds) *Hydrocarbon exploration and exploitation West of Shetlands*. Geological Society, London, Special Publications, **397**, 1–10.

Babechuk, M.G., Widdowson, M. & Kamber, B.S. 2014. Quantifying chemical weathering intensity and trace element release from two contrasting basalt profiles, Deccan Traps, India. *Chemical Geology*, **363**, 56-75.

Barker, A.K., Baker, J.A. & Peate, D.W. 2006. Interaction of the rifting East Greenland margin with a zoned ancestral Iceland plume. *Geology*, **34**, 481–484.

Bartetzko, A., Delius, H. & Pechnig, R. 2005. Effect of compositional and structural variations on log responses of igneous and metamorphic rocks. I: mafic rocks. *In:* Harvey, P.K., Brewer, T.S., Pezard, P.A. & Petrov, V.A. (eds) *Petrophysical Properties of Crystalline Rocks.* Geological Society, London, Special Publications, **240**, 255–278.

Boldreel, L.O. 2006. Wire-line log-based stratigraphy of flood basalts from the Lopra-1/1A well, Faroe Islands. *Geological Survey of Denmark and Greenland Bulletin*, **9**, 7–22.

Brodie, J.A. & Fitton, J.G. 1998. *Data report:* Composition of basaltic lavas from the seaward-dipping reflector sequence recovered during Deep Sea Drilling Project Leg 81 (Hatton Bank). *In:* Saunders, A.D., Larsen, H.C., & Wise, S.W., Jr. (eds.), *Proceedings of the Ocean Drilling Program, Scientific Results,* Vol. 152, College Station, Texas, (Ocean Drilling Program), 431–435.

Bryan, W.B. 1972. Morphology of quench crystals in submarine basalts. *Journal of Geophysical Research*, **77**, 5812–5819.

Dale, C.W., Pearson, D.G., Starkey, N.A., Stuart, F.M., Ellam, R.M., Larsen, L.M. Fitton, J.G. & Macpherson, C.G. 2008. Osmium isotopes in Baffin Island and West Greenland picrites: Implications for the $^{187}Os/^{188}Os$ composition of the convecting mantle and the nature of high $^{3}He/^{4}He$ mantle. *Earth and Planetary Science Letters*, **278,** 267–277.

Delpino, D.H. & Bermúdez, A.M. 2009. Petroleum systems including unconventional reservoirs in intrusive igneous rocks (sills and laccoliths). *The Leading Edge*, **28**, 804–811.

Doré, A.G., Lundin, E.R., Jensen, L.N., Birkeland, O., Eliassen, P.E. & Fichler, C. 1999. Principal tectonic events in the evolution of the northwest European Atlantic margin. *In:* Fleet, A.J. & Boldy, S.A.R. (eds) *Petroleum Geology of Northwest Europe - Proceedings of the 5th Conference.* Geological Society, London, Petroleum Geology Conference Series, **5**, 41–61.

Duncan, L., Helland-Hansen, D. & Dennehy, C. 2009. The Rosebank Discovery: A new play type in intra basalt reservoirs of the North Atlantic volcanic province. *6th European Production and Development Conference and Exhibition (DEVEX)*, Abstracts. Chevron Upstream Europe, Aberdeen.

Ebdon, C.C., Granger, P.J., Johnson, H.D. & Evans, A.M. 1995. Early Tertiary evolution and sequence stratigraphy of the Faeroe–Shetland Basin: implications for hydrocarbon prospectivity. *In:* Scrutton, R. A., Stoker, M. S., Shimmield, G. B. & Tudhope, A. W. (eds) *The Tectonics, Sedimentation and Palaeoceanography of the North Atlantic Region.* Geological Society, London, Special Publications, **90**, 51–69.

Ebinghaus, A., Hartley, A.J., Jolley, D.W., Hole, M.J. & Millett, J.M. 2014. Lava–Sediment Interaction and Drainage-System Development in a Large Igneous Province: Columbia River Flood Basalt Province, Washington State, U.S.A. *Journal of Sedimentary Research*, **84**, 1041–1063.

Fitton, J.G., Saunders, A.D., Norry, M.J., Hardarson, B.S. & Taylor R.N. 1997. Thermal and chemical structure of the Iceland plume. *Earth and Planetary Science Letters*, **153**, 197–208.

Fitton, J.G., Saunders, A.D., Larsen, H.C., Hardarson, B.S. & Norry, M.J. 1998. Volcanic rocks from the East Greenland margin at 63°N: composition, petrogenesis and mantle sources. *In:* Saunders, A.D., Larsen, H.C., Wise, S. & Allen, J.R. (eds) *Proceedings of the Ocean Drilling Program, Scientific Results,* **152**. Ocean Drilling Program, College Station, TX, 331–350.

Fletcher, R., Kusznir, N., Roberts, A. & Hunsdale, R. 2013. The formation of a failed continental breakup basin: The Cenozoic development of the Faroe-Shetland Basin. *Basin Research*, **25**, 532–553.

Gariepy, C., Ludden, J.N. & Brooks, C.K. 1983. Isotopic and trace element constraints on the genesis of the Faeroe lava pile. *Earth and Planetary Science Letters*, **63**, 257–272.

Gazel, E., Hoernle, K., Carr, M.J., Herzberg, C., Saginor, I., van den Bogaard, P., Feigensonm M. & Swisher III, C. 2011. Plume–subduction interaction in southern Central America: Mantle upwelling and slab melting. *Lithos,* **121**, 117-134.

Hald, N. & Waagstein, R. 1984. Lithology and chemistry of a 2-km sequence of Lower Tertiary tholeiitic lavas drilled on Suðuroy, Faeroe Islands (Lopra-1). *In:* Berthelsen, O., Noe-Nygaard, A. & Rasmussen, J. (eds) *The Deep Drilling Project 1980–1981 in the Faeroe Islands*. Tórshavn, Annales Societatis Scientiarum Færoensis, 15–38.

Hartley, R.A., Roberts, G.G., White, N. & Richardson, C. 2011. Transient convective uplift of an ancient buried landscape. *Nature Geoscience*, **4**, 562-565.

Helm-Clark, C.M., Rodgers, D.W. & Smith, R.P. 2004. Borehole geophysical techniques to define stratigraphy, alteration and aquifers in basalt. *Journal of Applied Geophysics*, **55**, 3–38.

Herzberg, C. 2004. Partial crystallization of mid-ocean ridge basalts in the crust and mantle. *Journal of Petrology*, **45**, 2389-2405.

Herzberg, C. & Asimow, P.D. 2015. PRIMELT3 MEGA.XLSM software for primary magma calculation: Peridotite primary magma MgO contents from the liquidus to the solidus. Technical Reports: methods, *Geochemistry, Geophysics, Geosystems*, **16**, 563-578.

Hole, M.J. 2015. The generation of continental flood basalts by decompression melting of internally heated mantle, *Geology*, **43,** 311–314.

Hole, M.J., Jolley, D.W., Hartley, A., Leleu, S., John, N. & Ball, M. 2013. Lava-sediment interactions in an Old Red Sandstone Basin, NE Scotland. *Journal of the Geological Society,* **170**, 641–645.

Hole, M.J., Millett, J.M., Jolley, D.W. & Rogers, N. 2015. Rifting and Mafic Magmatism in the Hebridean Basins. *Journal of the Geological Society, London*, online first.

Japsen, P., Andersen, C., *et al.* 2005. Preliminary results from investigations of seismic and petrophysical properties of Faroes basalts in the SeiFaBa project. In: Doré, A.G. & Vining, B.A. (eds) *Petroleum Geology: North-West Europe and Global Perspectives—Proceedings of the 6th Conference*, Geological Society, London, 1461–1470.

Jerram, D.A. 2002. Volcanology and facies architecture of flood basalts. *In:* Menzies, M. A., Klemperer, S.L., Ebinger, C.J. & Baker, J. (eds) *Volcanic Rifted Margins*. Geological Society of America, Special Paper, **362**, 119–132.

Jolley, D.W. 2009. Palynofloral evidence for the onset and cessation of eruption of the Faroe Islands lava field. *In:* Varming, T. & Ziska, H. (eds) *Faroe Islands Exploration Conference: Proceedings of the 2nd Conference. Annales Societatis Scientiarum, Færoensis, Supplementum*, **50**, 156–173.

Jolley, D.W., Passey, S.R., Hole, M.J. & Millett, J.M. 2012. Large-scale magmatic pulses drive plant ecosystem dynamics. *Journal of the Geological Society*, **169**, 703–711.

Jolley, D.W. & Bell, B.R. 2002a. The evolution of the North Atlantic Igneous Province and the opening of the NE Atlantic rift. *In:* Jolley, D.W. & Bell, B.R. (eds) *The North Atlantic Igneous Province. Stratigraphy, Tectonic, Volcanic and Magmatic Processes.* Geological Society, London, Special Publications, **197**, 1–13.

Jolley, D.W. & Bell, B.R. 2002b. Genesis and age of the Erland Volcano, NE Atlantic Margin. *In:* Jolley, D.W. & Bell, B.R. (eds) *The North Atlantic Igneous Province. Stratigraphy, Tectonic, Volcanic and Magmatic Processes.* Geological Society, London, Special Publications, **197**, 95–109.

Kanaris-Sotiriou, R., Morton, A.C. & Taylor, P.N. 1993. Palaeogene peraluminous magmatism, crustal melting and continental breakup: the Erlend complex, Faeroe-Shetland Basin, NE Atlantic. *Journal of the Geological Society*, *London*, 150, 903–914.

Kerr, A.C., Kent, R.W., Thompson, B.A., Seedhouse, J.K. & Donaldson, C.H. 1999. Geochemical Evolution of the Tertiary Mull Volcano, Western Scotland. *Journal of Petrology*, **40 (6)**, 873–908.

Larsen, H.C. & Saunders, A.D. 1998. Tectonism and volcanism at the southeast Greenland rifted margin: a record of plume impact and later continental rupture. *In:* Saunders, A.D., Larsen, H.C. & Wise, W.S. (eds) *Proceedings of the Ocean Drilling Program, Scientific Results*, **152**. Ocean Drilling Program, College Station, TX, 503–533.

Larsen, L.M. & Pedersen, A.K. 2009. Petrology of the Palaeocene picrites and flood basalts on Disko and Nuussuaq, West Greenland. *Journal of Petrology*, **50**, 1667–1711.

Larsen, L.M., Waagstein, R., Pedersen, A. K. & Storey, M. 1999. Trans-Atlantic correlation of the Palaeogene volcanic successions in the Faeroe Islands and East Greenland. *Journal of the Geological Society*, **156**, 1081–1095.

Lawver, L.A. & Müller, R.D. 1994. The Iceland hotspot track. *Geology*, **22**, 311–314.

Manghnani, M.H. & Woollard, G.P. 1965. Ultra-sonic velocities and related elastic properties of Hawaiian basaltic rocks. *Pacific Science*, **19**, 291–295.

Maynard, J.B. 1992. Chemistry of modern soils as a guide to interpreting Precambrian paleosols. *Journal of Geology*, **100**, 279–289.

Millett, J.M., Hole, M.J. & Jolley, D.W. 2014. A fresh approach to ditch cutting analysis as an aid to exploration in areas affected by large igneous province (LIP) volcanism. *In:* Cannon, S.J.C. & Ellis, D. (eds) *Hydrocarbon exploration and exploitation West of Shetlands*. Geological Society, London, Special Publications, **397**,193–207.

Millett, J.M. 2014. *Unpublished PhD thesis*. University of Aberdeen.

Morrison, M.A. 1978. The use of 'immobile' trace elements to distinguish the palaeotectonic affinities of metabasalts: applications to the Palaeocene basalts of Mull and Skye, NW Scotland. *Earth and Planetary Science Letters,* **39,** 407–416.

Morton, A.C., Dixon, J.E., Fitton, J.G., Macintyre, R.M., Smythe, D.K. & Taylor, P.N. 1988. Early Tertiary volcanic rocks in Well 163/6-1A, Rockall Trough. *In:* Morton, A.C. & Parson, L.M. (eds), *Early Tertiary Volcanism and the Opening of the NE Atlantic,* Geological Society Special Publication, **39**, 293–308.

Morton, A.C. & Keene, J. 1984. Paleogene pyroclastic volcanism in the southwest Rockall Plateau. *In:* Roberts, D.G., Schnitker, D., *et al. Initial Reports of the DSDP*, **81**, Washington (U.S. Govt. Printing Office), 633–643.

Mudge, D.C. & Jones, S.M. 2004. Palaeocene uplift and subsidence events in the Scotland-Shetland and North Sea region and their relationship to the Iceland Plume. *Journal of the Geological Society*, **161**, 381–386.

Murton, B.J., Taylor, R.N. & Thirlwall, M.F. 2002. Plume-ridge interaction: a geochemical perspective from the Reykjanes Ridge. *Journal of Petrology*, **43**, 1155–1176.

Nadin, P.A., Kusznir, N.J. & Cheadle, M.J. 1997. Early Tertiary plume uplift of the North Sea and Faeroe-Shetland Basins. *Earth and Planetary Science Letters*, **148**, 109–127.

Naylor, P.H., Bell, B.R., Jolley, D.W., Durnall, P. & Fredsted, R. 1999. Palaeogene magmatism in the Faeroe-Shetland Basin: influences on uplift history and sedimentation. *In:* Fleet, A.J. & Boldy, S.A.R. (eds) *Petroleum Geology of Northwest Europe, Proceedings of the 5th Conference.* Geological Society, London*, 545–558.*

Nelson, C.E., Jerram, D.A. & Hobbs, R.W. 2009a. Flood basalt facies from borehole data: implications for prospectivity and volcanology in volcanic rifted margins. *Petroleum Geoscience*, **15**, 313–324.

Nelson, C.E., Jerram, D.A., Single, R.T. & Hobbs, R.W. 2009b. Understanding the facies architecture of flood basalts and volcanic rifted margins and its effect on geophysical properties. *In:* Varming, T. & Ziska, H. (eds) *Faroe Islands Exploration Conference: Proceedings of the 2nd Conference*. *Annales Societatis Scientiarum Færoensis, Supplementum*, **50**, 84–103.

Nesbitt, H.W. & Wilson, R.E. 1992. Recent chemical weathering of basalts. *American Journal of Science*, **292**, 740-777.

Parson, L., Vierek, L., Love, D., Gibson, I.L., Morton A.C. & Hertogen, J. 1989. Petrology of the Lower Series volcanics, ODP site 642. In: Eldholm, O., Thiede, J., Taylor, E. *et al.*

(eds) *Proceedings of the Ocean Drilling Program, Scientific Results*, Vol **104**, College Station Texas (Ocean Drilling Program) 419-428.

Passey, S.R. 2004. *Unpublished PhD Thesis*. University of Glasgow.

Passey, S.R. & Jolley, D.W. 2009. A revised lithostratigraphic nomenclature for the Palaeogene Faroe Islands Basalt Group, NE Atlantic Ocean. *Earth and Environmental Science Transactions of the Royal Society of Edinburgh*, **99**, 127–158.

Pedersen, A.K., Watt, M., Watt, W.S. & Larsen, L.M. 1997. Structure and stratigraphy of the Early Tertiary basalts of the Blosseville Kyst, East Greenland. *Journal of the Geological Society,* **154**, 565–570.

Planke, S. & Cambray, H. 1998. Seismic properties of flood basalts from hole 917A downhole data, southeast Greenland volcanic margin. *In:* Saunders, A.D., Larsen, H.C., and Wise, S.W., Jr. (eds.), *Proceedings of the Ocean Drilling Program, Scientific Results,* Vol. 152, College Station, Texas, (Ocean Drilling Program), 453–462.

Planke, S. 1994. Geophysical response of flood basalts from analysis of wire line logs: Ocean Drilling Program Site 642, Vøring volcanic margin. *Journal of Geophysical Research*, **99**, 9279–9296.

Planke, S., Alvestad, E. & Eldholm, O. 1999b. Seismic characteristics of basaltic extrusive and intrusive rocks. *The Leading Edge*, **18**, 342–348.

Planke, S., Cerney, B. & Nilsen, O. 1999a. Alteration effects on petrophysical properties of subaerial flood basalts: Site 990, Southeast Greenland Margin. *In:* Larsen, H.C., Duncan, R.A., Allan, J.F. & Brooks, K. (eds) *Proceedings of the Ocean Drilling Program, Scientific Results*, Vol. 163. Texas, Ocean Drilling Program, 17–28.

Planke, S., Symonds, P.A., Alvestad, E. & Skogseid, J. 2000. Seismic volcanostratigraphy of large-volume basaltic extrusive complexes on rifted margins. *Journal of Geophysical Research*, **105**, 19335–19351.

Putirka, K.D., Perfit, M., Ryerson, F.J. & Jackson, M.G. 2007.Ambient and excess mantle temperatures, olivine thermometry, andactive vs. passive upwelling. *Chemical Geology*, **24**, 177-206.

Rateau, R., Schofield, N., & Smith, M., 2013. The potential role of igneous intrusions on hydrocarbon migration, West of Shetland. *Petroleum Geoscience*, **19**, 259–272.

Saunders, A.D., Fitton, J.G., Kerr, A.C., Norry, M.J. & Kent, R.W. 1997. The North Atlantic Igneous Province. *In:* Mahoney, J.J. & Coffin, M.F. (eds) *Large Igneous Provinces. Geophysical Monograph, American Geophysical Union*, **100**, 45–94.

Saunders, A.D., Jones, S.M., Morgan, L.A., Pierce, K.L., Widdowson, M. & Xu, Y.G. 2007. Regional uplift associated with continental large igneous provinces: the roles of mantle plumes and the lithosphere. *Chemical Geology*, **241**, 282–318.

Schofield, N. & Jolley, D.W. 2013. Development of intra-basaltic lava-field drainage systems within the Faroe-Shetland Basin. *Petroleum Geoscience*, **19**, 273–288.

Shaw Champion, M.E., White, N.J., Jones, S.M. & Lovell, J.P.B. 2008. Quantifying transient mantle convective uplift: An example from the Faroe-Shetland basin. *Tectonics*, **27**, TC1002.

Skilling, I.P. 2002. Basaltic pahoehoe-fed lava deltas; large-scale characteristics, clast generation, emplacement processes and environmental discrimination. *In:* Smellie, J. L. & Chapman, M. G. (eds). *Volcano-Ice Interaction on Earth and Mars.* Geological Society, London, Special Publications, **202**, 91–113.

Søager, N., Holm, P.M., 2009. Extended correlation of the Paleogene Faroe Islands and East Greenland plateau basalts. *Lithos,* **107 (3–4)**, 205–215.

Søager, N. & Holm P.M. 2011. Changing compositions in the Iceland plume; Isotopic and elemental constraints from the Paleogene Faroe flood basalts. *Chemical Geology*, **280**, 297–313.

Starkey, A.A., Stuart, F.M., Ellam, R.M., Fitton J.G., S, Basu & Larsen L.M. 2009. Helium isotopes in early Iceland plume picrites: constraints on the composition of high $^{3}He/^{4}He$ mantle. *Earth and Planetary Science Letters*, **277**, 91–100.

Storey, M., Duncan, R.A., Pedersen, A.K., Larsen, L.M. & Larsen, H.C. 1998. $^{40}Ar/^{39}Ar$ geochronology of the West Greenland Tertiary volcanic province. *Earth and Planetary Science Letters*, **160**, 569–586.

Stracke, A., Zindler, A., Salters, V.J.M., McKenzie, D., Blichert-Toft, J., Albarède, F. & Grönvold, K. 2003. Theistareykir revisited. *Geochemistry, Geophysics, Geosystems*, **4**, 1–49.

Thompson, R.N. 1982. Magmatism of the British Tertiary Volcanic Province. *Scottish Journal of Geology*, **18**, 49–107.

Vierek, L.G., Hertogen, J., Parson, L.M., Morton, A.C., Love, D., & Gibson, I.L. 1989. Chemical stratigraphy and petrology of the Voring Plateau tholeiitic lavas and interlayered volcaniclastic sediments at ODP Hole 642E. *In:* Eldholm, O., Thiede, J., Taylor, E. *et al.* (eds) *Proceedings of the Ocean Drilling Program, Scientific Results*, **104**, College Station Texas (Ocean Drilling Program), 367–396.

Waight, T.E. & Baker, J.A. 2012. Depleted Basaltic Lavas from the Proto-Iceland Plume, Central East Greenland. *Journal of Petrology*, **53**, 1569–1596.

Watton, T.J., Cannon, S., Brown, R. J., Jerram, D. A. & Waichel, B. L. 2014a. Using Formation Micro Imaging, Wireline logs and Onshore Analogues to Distinguish Volcanic Lithofacies in Boreholes: Examples from Palaeogene Successions in the Faroe-Shetland Basin, Northeast Atlantic. *In:* Cannon, S. & Ellis, D. (eds) *Exploration to Exploitation West of Shetlands. Geological Society, London, Special Publications,* **397**, 173–192.

Watton, T.J., Jerram, D.A., Thordarson, T. & Davies, R.J. 2013. Three-dimensional lithofacies variations in hyaloclastite deposits. *Journal of Volcanology and Geothermal Research*, **250**, 19–33.

Watton, T.J., Wright, K.A., Jerram, D.J. & Brown, R.J. 2014b. The petrophysical and petrographical properties of hyaloclastite deposits: Implications for petroleum exploration. *AAPG Bulletin*, **98(3)**, 449–463.

Wood, D.A., Varet, J., Bougault. H., *et al.* 1979. The petrology, geochemistry and mineralogy of North Atlantic basalts. A discussion based on IPOD Leg 49. *In:* Luyendyk, B.P., Cann. J.R., *et al.* (eds). *Initial Reports of the DSDP*, **49**, Washington (U.S. Govt. Printing Office), 597–655.

Wright K.A., Davies, R.J., Jerram, D.A., Morris, J. & Fletcher, R. 2012. Application of seismic and sequence stratigraphic concepts to a lava-fed delta system in the Faroe-Shetland Basin, UK and Faroes. *Basin Research,* **24**, 91–106.

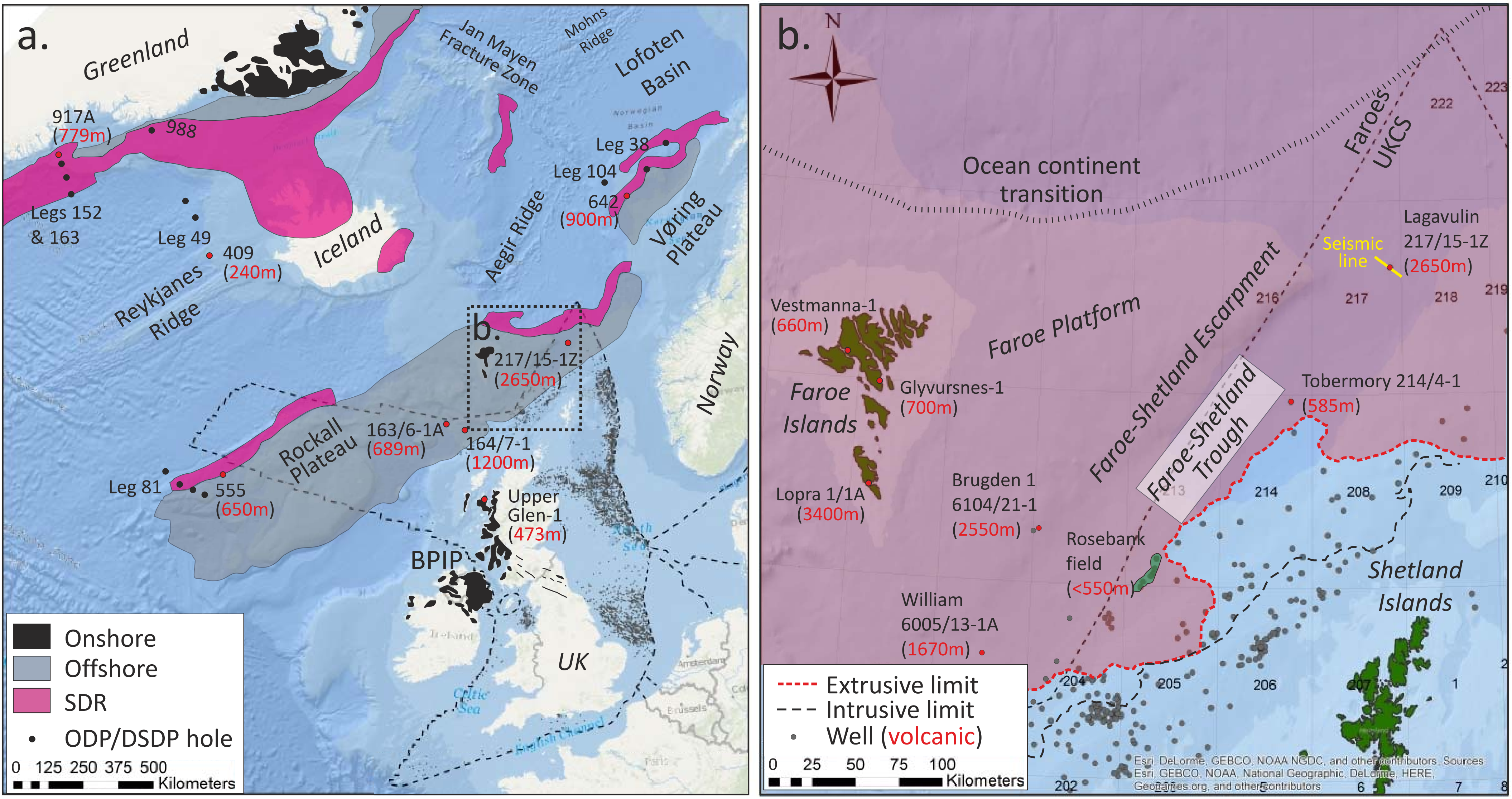
a.
Greenland
917A
(779m)
988
Legs 152
& 163
Leg 49
409
(240m)
Iceland
Reykjanes
Ridge
Jan Mayen
Fracture Zone
Mohns
Ridge
Aegir Ridge
Lofoten
Basin
Leg 38
Leg 104
642
(900m)
Vøring
Plateau
Norway
b.
217/15-1Z
(2650m)
163/6-1A
(689m)
164/7-1
(1200m)
Rockall
Plateau
Leg 81
555
(650m)
Upper
Glen-1
(473m)
BPIP
UK
Onshore
Offshore
SDR
ODP/DSDP hole
0 125 250 375 500
Kilometers
b.
N
Ocean continent
transition
Faroes
UKCS
Lagavulin
217/15-1Z
(2650m)
Seismic
line
Faroe Platform
Faroe-Shetland Escarpment
Faroe-Shetland
Trough
Vestmanna-1
(660m)
Faroe
Islands
Glyvursnes-1
(700m)
Lopra 1/1A
(3400m)
Brugden 1
6104/21-1
(2550m)
Tobermory 214/4-1
(585m)
Rosebank
field
(<550m)
William
6005/13-1A
(1670m)
Shetland
Islands
Extrusive limit
Intrusive limit
Well (volcanic)
0 25 50 75 100
Kilometers
Esri, DeLorme, GEBCO, NOAA NGDC, and other contributors, Sources: Esri, GEBCO, NOAA, National Geographic, DeLorme, HERE, Geonames.org, and other contributors

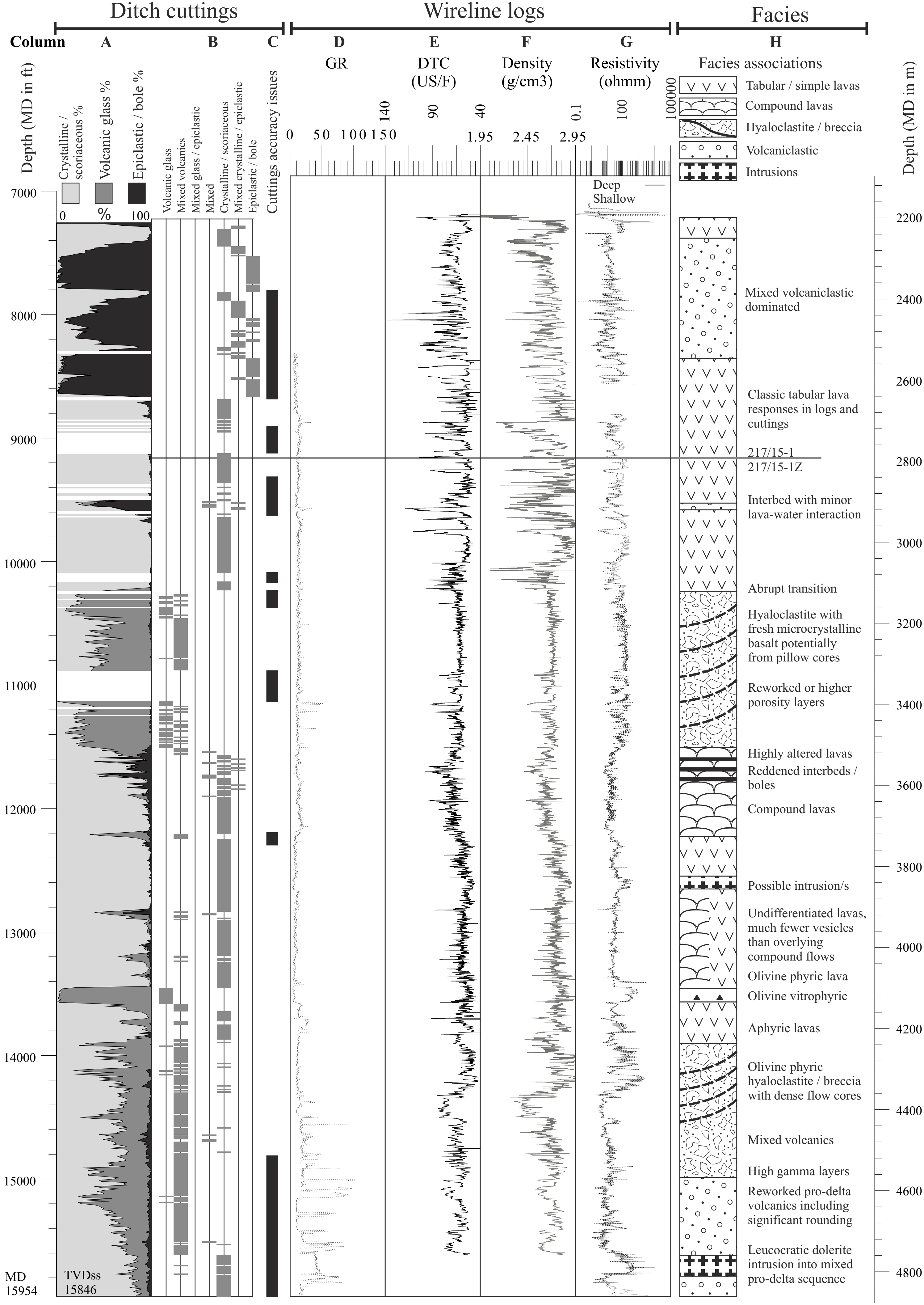

Ditch cuttings
Wireline logs
Facies
Column A B C D E F G H
Depth (MD in ft)
Crystalline / scoriaceous %
Volcanic glass %
Epiclastic / bole %
0 % 100
Volcanic glass
Mixed volcanics
Mixed glass / epiclastic
Mixed
Crystalline / scoriaceous
Mixed crystalline / epiclastic
Epiclastic / bole
Cuttings accuracy issues
GR
0 50 100 150
DTC (US/F)
140 90 40
Density (g/cm3)
1.95 2.45 2.95
Resistivity (ohmm)
0.1 100 100000
Deep
Shallow
Facies associations
Tabular / simple lavas
Compound lavas
Hyaloclastite / breccia
Volcaniclastic
Intrusions
Depth (MD in m)
7000 8000 9000 10000 11000 12000 13000 14000 15000
MD 15954
TVDss 15846
2200 2400 2600 2800 3000 3200 3400 3600 3800 4000 4200 4400 4600 4800
Mixed volcaniclastic dominated
Classic tabular lava responses in logs and cuttings
217/15-1
217/15-1Z
Interbed with minor lava-water interaction
Abrupt transition
Hyaloclastite with fresh microcrystalline basalt potentially from pillow cores
Reworked or higher porosity layers
Highly altered lavas
Reddened interbeds / boles
Compound lavas
Possible intrusion/s
Undifferentiated lavas, much fewer vesicles than overlying compound flows
Olivine phyric lava
Olivine vitrophyric
Aphyric lavas
Olivine phyric hyaloclastite / breccia with dense flow cores
Mixed volcanics
High gamma layers
Reworked pro-delta volcanics including significant rounding
Leucocratic dolerite intrusion into mixed pro-delta sequence

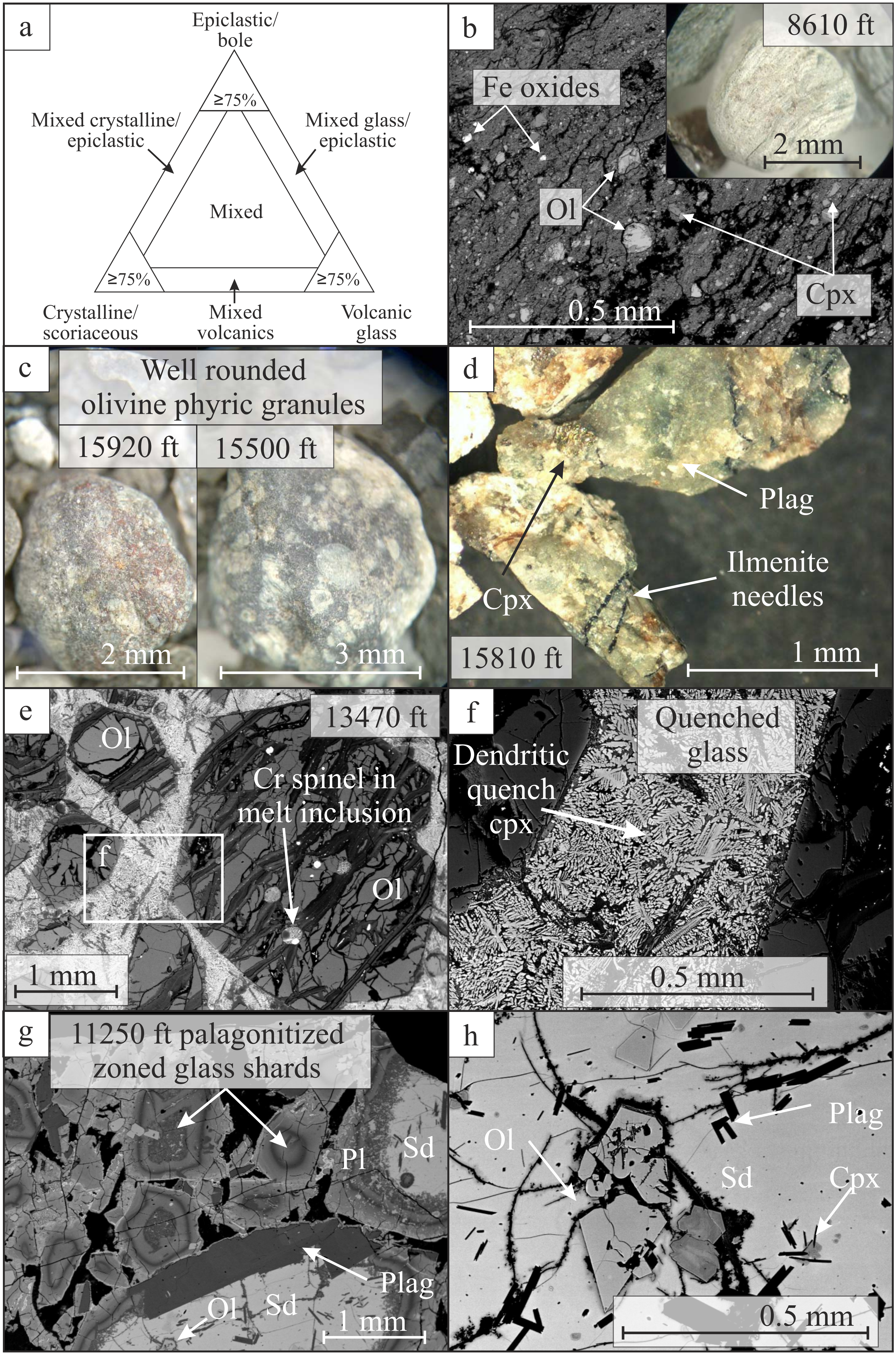
a
Epiclastic/
bole
≥75%
Mixed crystalline/
epiclastic
Mixed glass/
epiclastic
Mixed
≥75%
≥75%
Crystalline/
scoriaceous
Mixed
volcanics
Volcanic
glass
b
8610 ft
Fe oxides
2 mm
Ol
Cpx
0.5 mm
c
Well rounded
olivine phyric granules
15920 ft
15500 ft
2 mm
3 mm
d
Plag
Cpx
Ilmenite
needles
15810 ft
1 mm
e
13470 ft
Ol
Cr spinel in
melt inclusion
f
Ol
1 mm
f
Quenched
glass
Dendritic
quench
cpx
0.5 mm
g
11250 ft palagonitized
zoned glass shards
Pl
Sd
Plag
Ol
Sd
1 mm
h
Ol
Plag
Sd
Cpx
0.5 mm

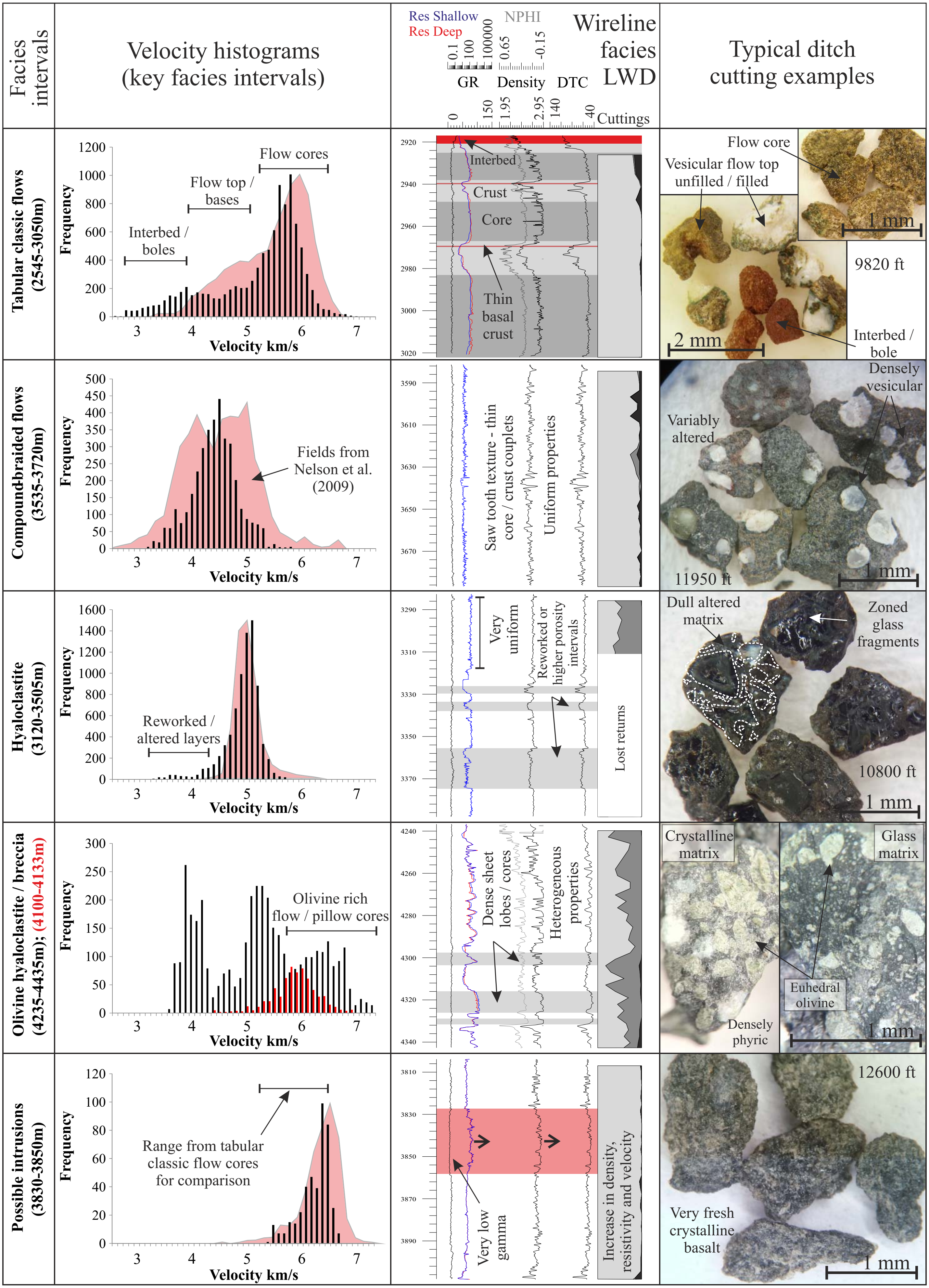

Facies intervals
Velocity histograms (key facies intervals)
Res Shallow
Res Deep
NPHI
0.1
100
100000
0.65
-0.15
GR
Density
DTC
0
150
1.95
2.95
140
40
Cuttings
Wireline facies LWD
Typical ditch cutting examples
Tabular classic flows (2545-3050m)
Frequency
Velocity km/s
Flow cores
Flow top / bases
Interbed / boles
Interbed
Crust
Core
Thin basal crust
Flow core
Vesicular flow top unfilled / filled
1 mm
9820 ft
2 mm
Interbed / bole
Compound-braided flows (3535-3720m)
Fields from Nelson et al. (2009)
Saw tooth texture - thin core / crust couplets
Uniform properties
Densely vesicular
Variably altered
11950 ft
1 mm
Hyaloclastite (3120-3505m)
Reworked / altered layers
Very uniform
Reworked or higher porosity intervals
Lost returns
Dull altered matrix
Zoned glass fragments
10800 ft
1 mm
Olivine hyaloclastite / breccia (4235-4435m); (4100-4133m)
Olivine rich flow / pillow cores
Dense sheet lobes / cores
Heterogeneous properties
Crystalline matrix
Glass matrix
Euhedral olivine
Densely phyric
1 mm
Possible intrusions (3830-3850m)
Range from tabular classic flow cores for comparison
Very low gamma
Increase in density, resistivity and velocity
12600 ft
Very fresh crystalline basalt
1 mm

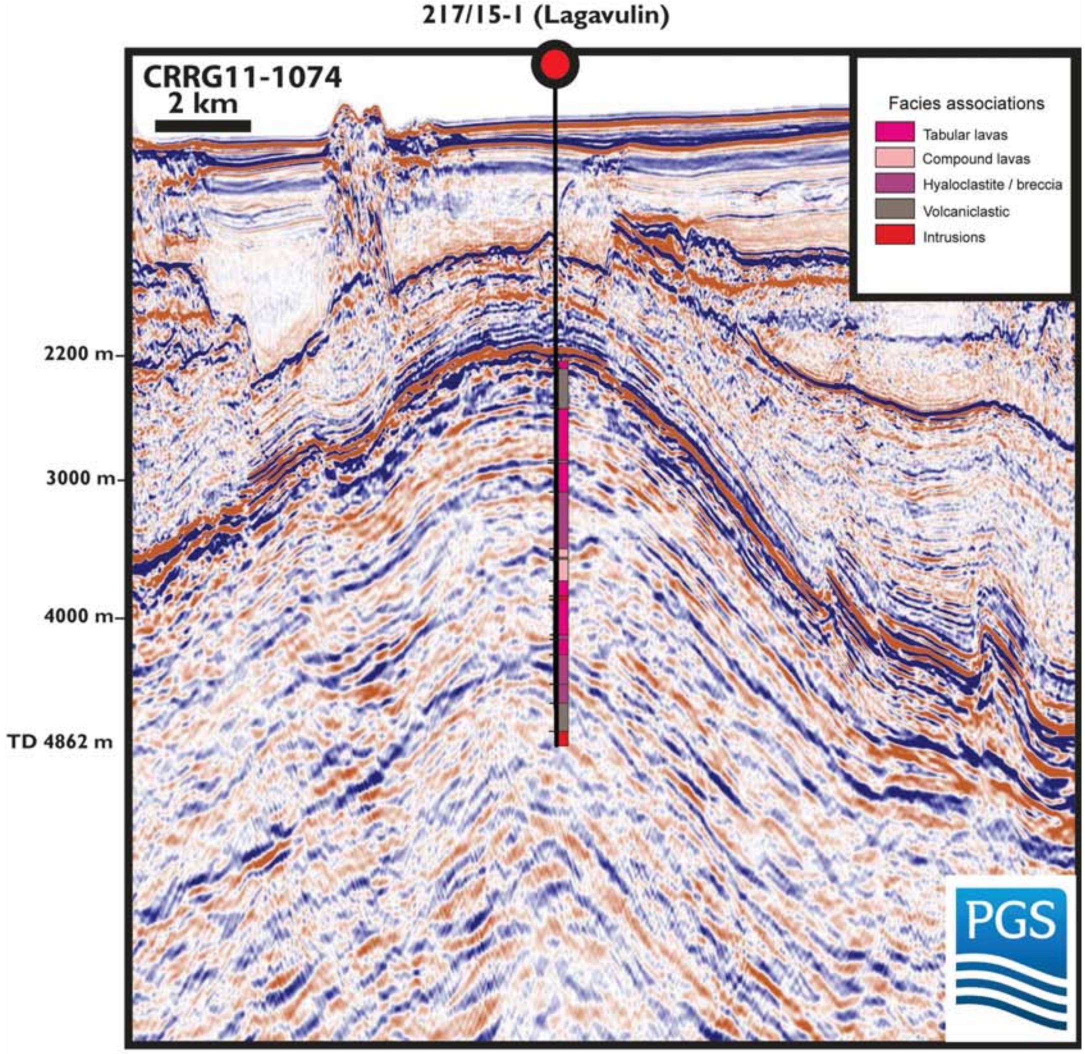
217/15-1 (Lagavulin)
CRRG11-1074
2 km
Facies associations
Tabular lavas
Compound lavas
Hyaloclastite / breccia
Volcaniclastic
Intrusions
2200 m
3000 m
4000 m
TD 4862 m
PGS

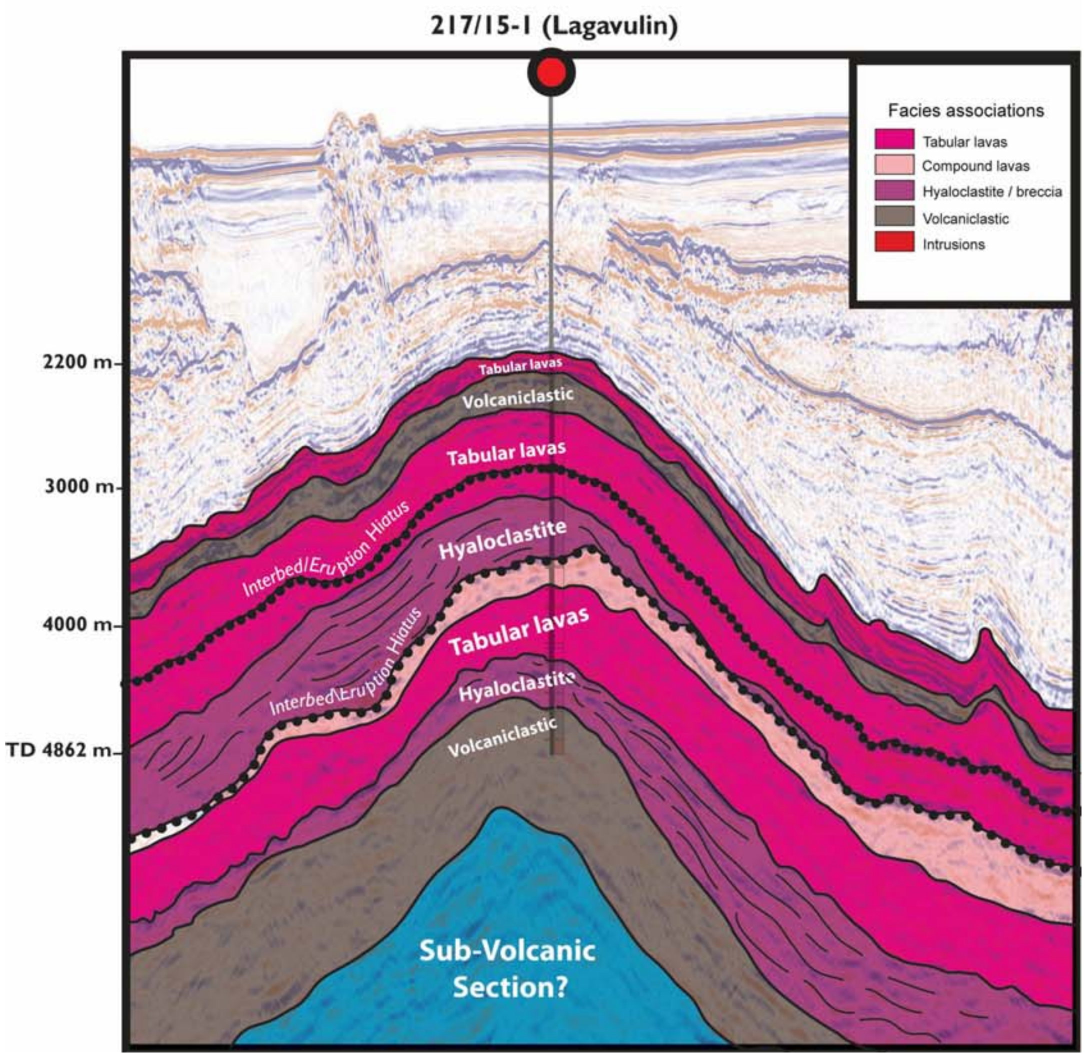
217/15-1 (Lagavulin)
Facies associations
Tabular lavas
Compound lavas
Hyaloclastite / breccia
Volcaniclastic
Intrusions
2200 m
3000 m
4000 m
TD 4862 m
Tabular lavas
Volcaniclastic
Tabular lavas
Interbed/Eruption Hiatus
Hyaloclastite
Interbed\Eruption Hiatus
Tabular lavas
Hyaloclastite
Volcaniclastic
Sub-Volcanic Section?

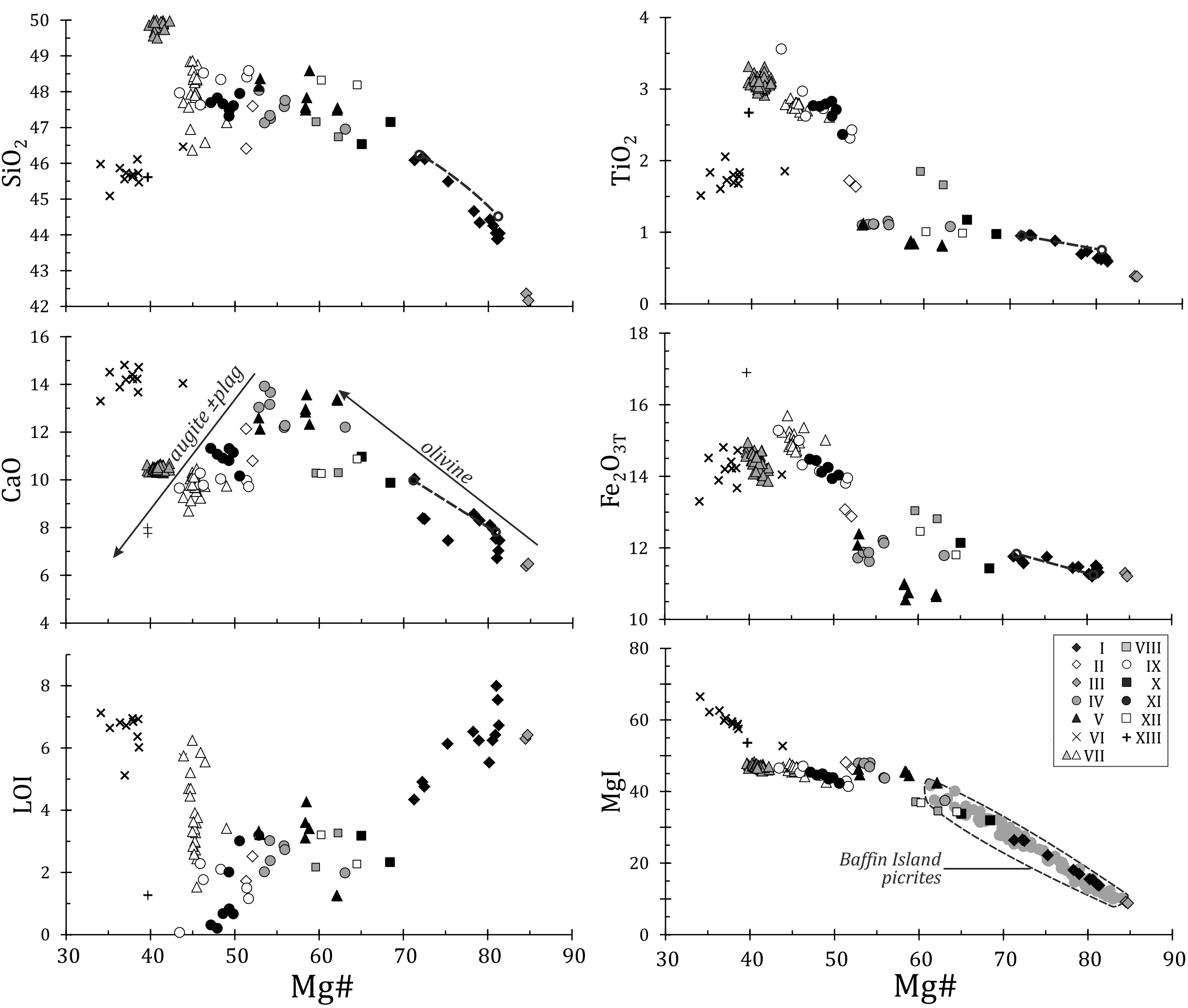

SiO2
TiO2
CaO
Fe2O3T
LOI
MgI
Mg#
augite ±plag
olivine
Baffin Island picrites
I
II
III
IV
V
VI
VII
VIII
IX
X
XI
XII
XIII

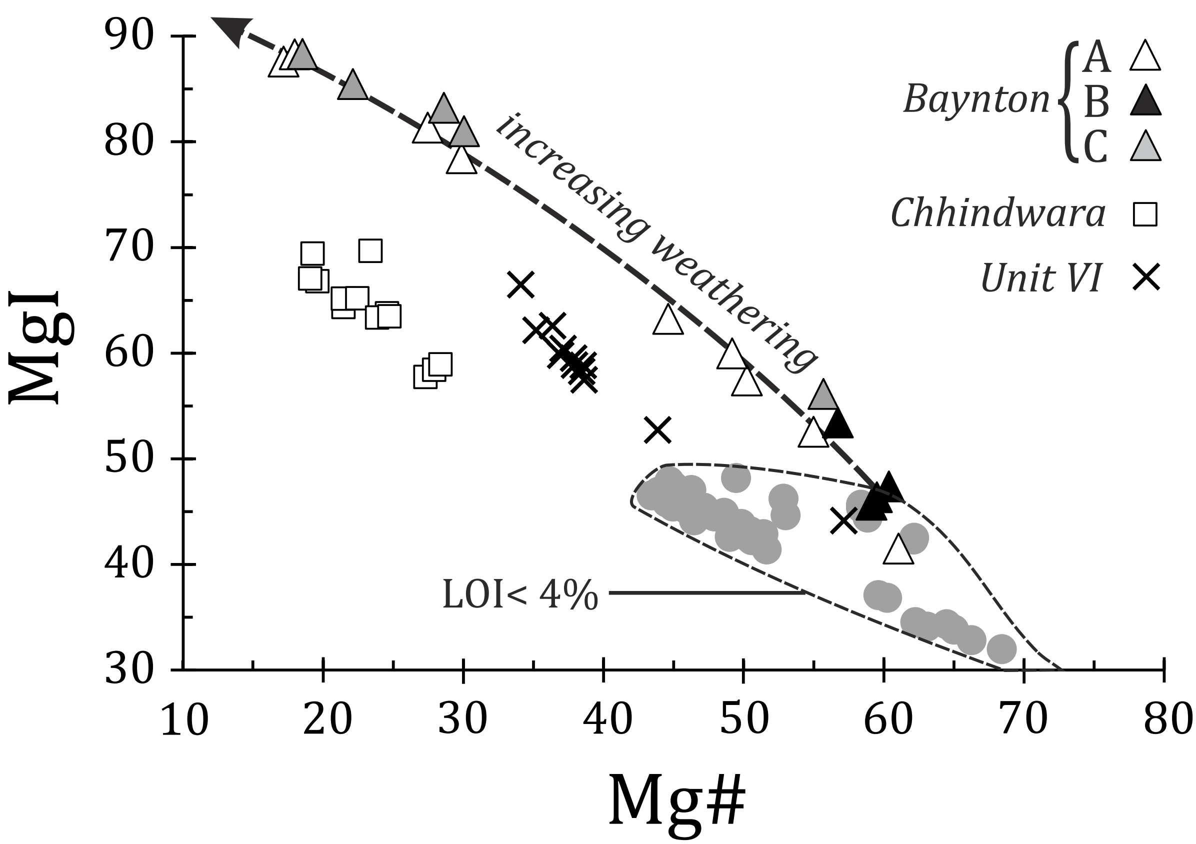

90
80
70
60
50
40
30
10
20
30
40
50
60
70
80
Mg#
MgI
increasing weathering
LOI< 4%
Baynton
A
B
C
Chhindwara
Unit VI

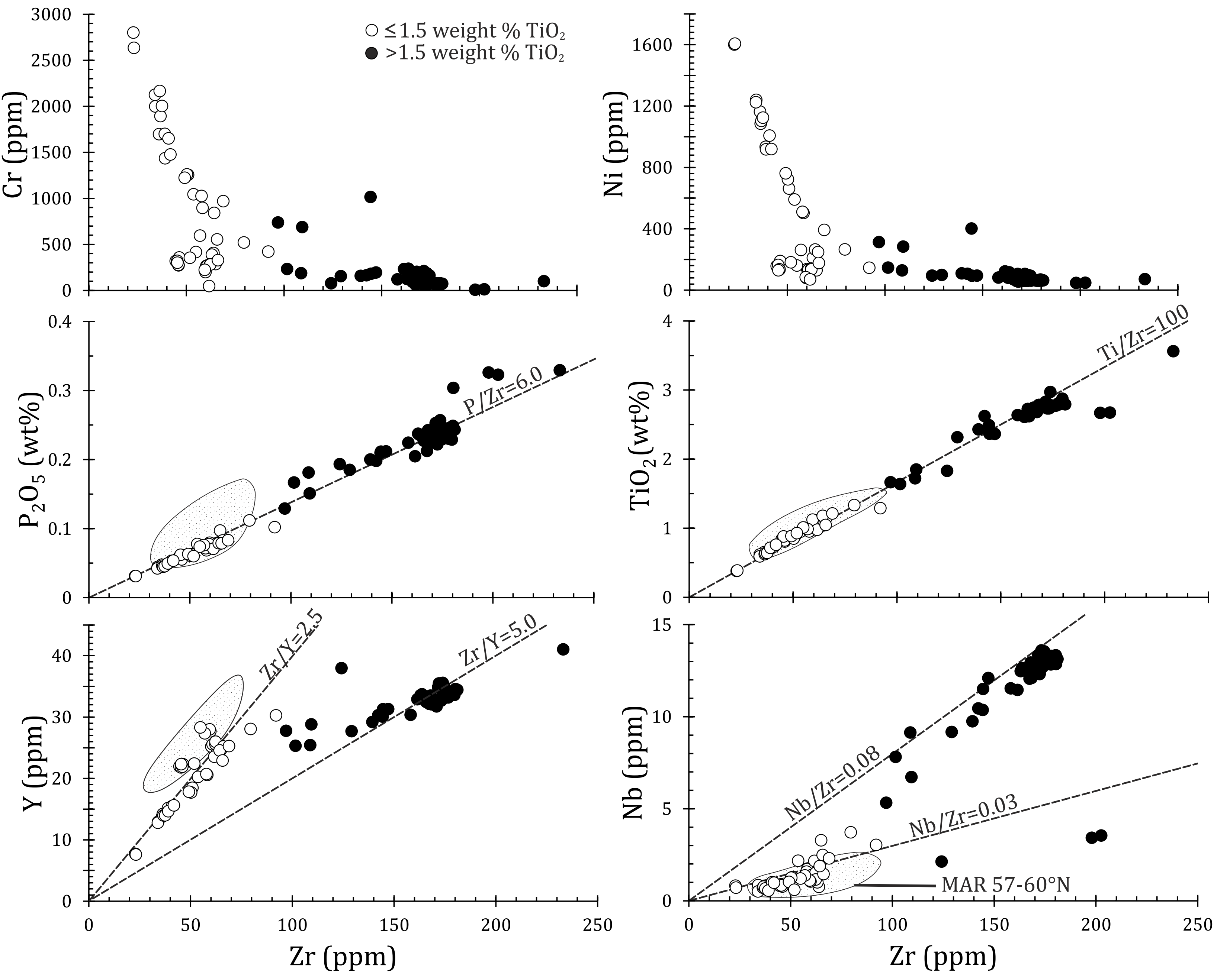

≤1.5 weight % TiO2
>1.5 weight % TiO2
Cr (ppm)
Ni (ppm)
P2O5 (wt%)
P/Zr=6.0
TiO2 (wt%)
Ti/Zr=100
Y (ppm)
Zr/Y=2.5
Zr/Y=5.0
Nb (ppm)
Nb/Zr=0.08
Nb/Zr=0.03
MAR 57-60°N
Zr (ppm)
Zr (ppm)

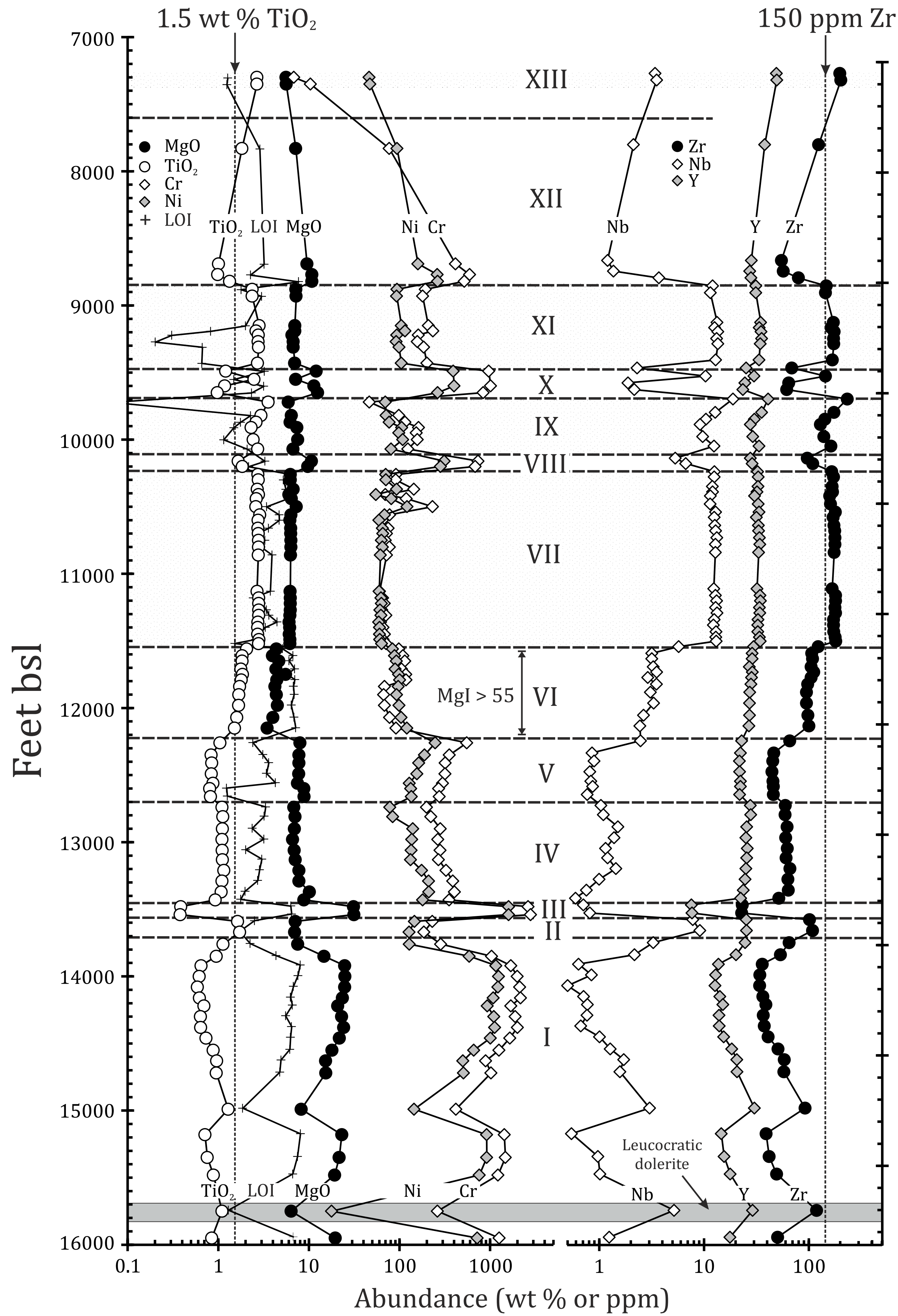
1.5 wt % TiO2
150 ppm Zr
Feet bsl
Metres bsl
MgO
TiO2
Cr
Ni
LOI
Zr
Nb
Y
XIII
XII
XI
X
IX
VIII
VII
VI
MgI > 55
V
IV
III
II
I
Leucocratic dolerite
Abundance (wt % or ppm)

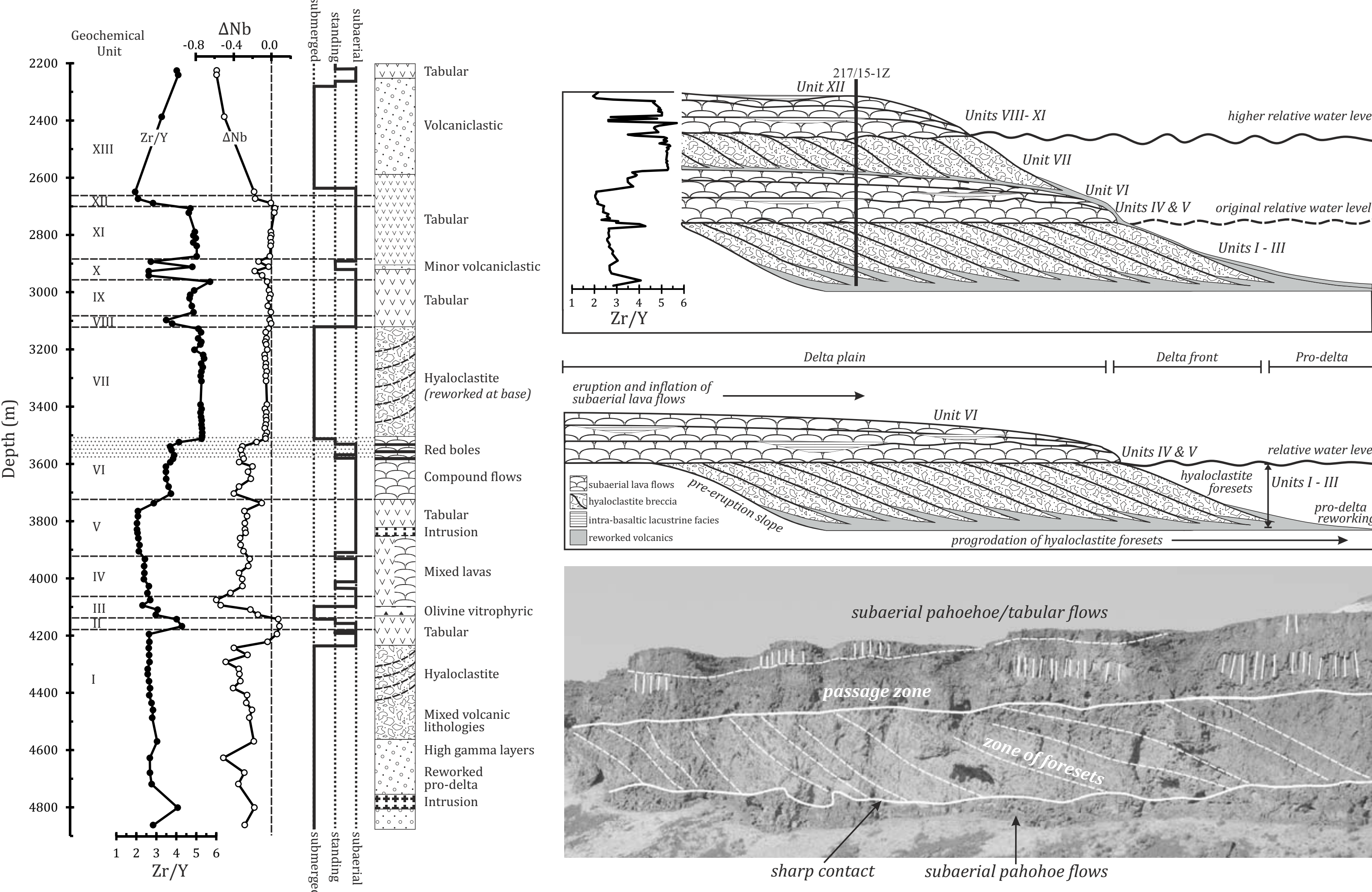

Geochemical Unit
ΔNb
-0.8 -0.4 0.0
submerged
standing
subaerial
Depth (m)
2200
2400
2600
2800
3000
3200
3400
3600
3800
4000
4200
4400
4600
4800
XIII
XII
XI
X
IX
VIII
VII
VI
V
IV
III
II
I
Zr/Y
ΔNb
1 2 3 4 5 6
Zr/Y
Tabular
Volcaniclastic
Tabular
Minor volcaniclastic
Tabular
Hyaloclastite
(reworked at base)
Red boles
Compound flows
Tabular
Intrusion
Mixed lavas
Olivine vitrophyric
Tabular
Hyaloclastite
Mixed volcanic lithologies
High gamma layers
Reworked pro-delta
Intrusion
217/15-1Z
Unit XII
Units VIII- XI
higher relative water level
Unit VII
Unit VI
Units IV & V
original relative water level
Units I - III
1 2 3 4 5 6
Zr/Y
Delta plain
Delta front
Pro-delta
eruption and inflation of subaerial lava flows
Unit VI
Units IV & V
relative water level
hyaloclastite foresets
Units I - III
subaerial lava flows
hyaloclastite breccia
intra-basaltic lacustrine facies
reworked volcanics
pre-eruption slope
pro-delta reworking
progradation of hyaloclastite foresets
subaerial pahoehoe/tabular flows
passage zone
zone of foresets
~40m
sharp contact
subaerial pahoehoe flows

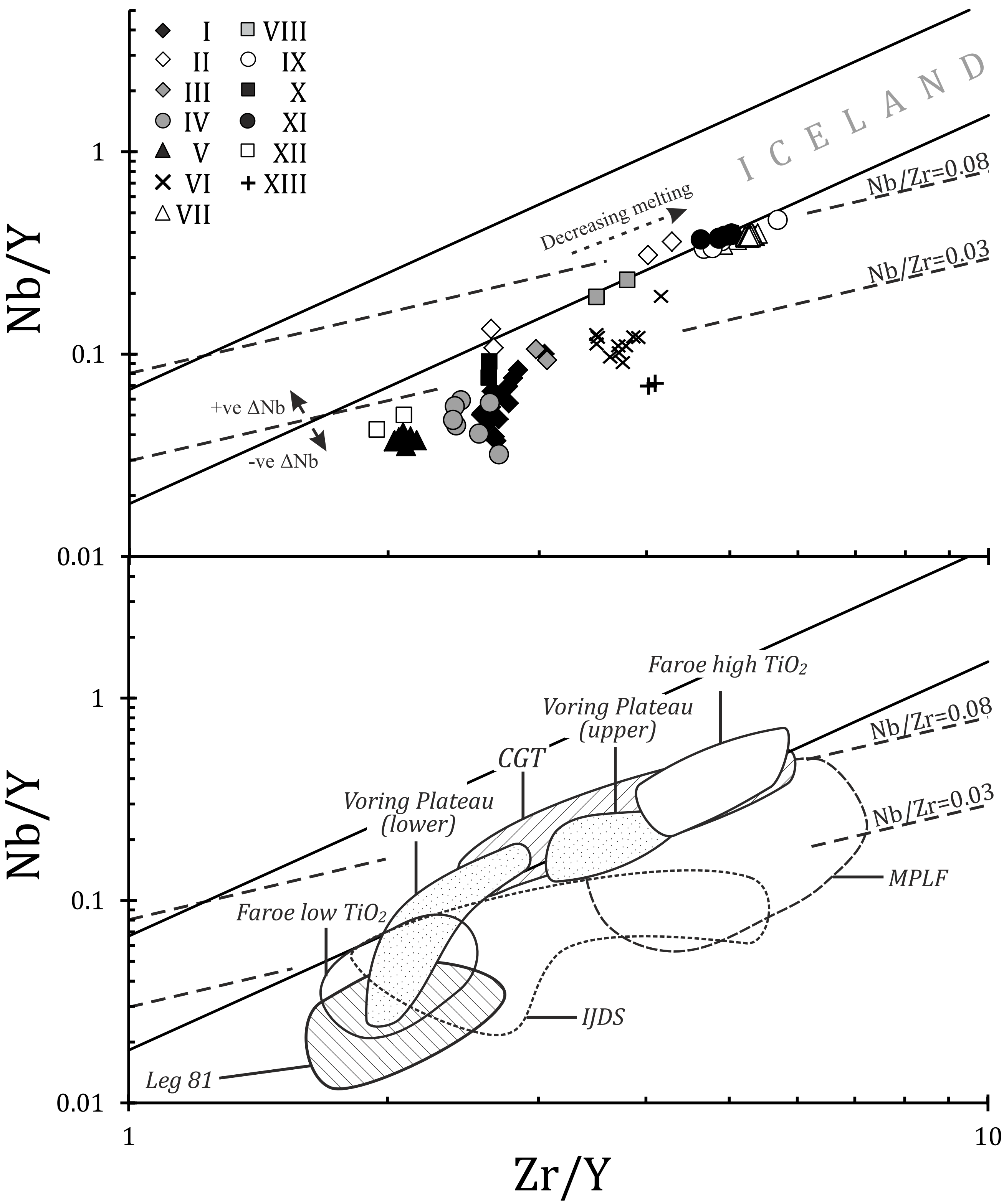

I
II
III
IV
V
VI
VII
VIII
IX
X
XI
XII
XIII
ICELAND
Decreasing melting
Nb/Zr=0.08
Nb/Zr=0.03
+ve ΔNb
-ve ΔNb
Nb/Y
1
0.1
0.01
Faroe high TiO2
Voring Plateau (upper)
CGT
Voring Plateau (lower)
Faroe low TiO2
MPLF
IJDS
Leg 81
10
Zr/Y